Science of the Total Environment 904 (2023) 167532

Contents lists available at ScienceDirect

Science of the Total Environment

journal homepage: www.elsevier.com/locate/scitotenv

Mercury mobilization in shrubland after a prescribed fire in NE Portugal: Insight on soil organic matter composition and different aggregate size

Melissa Méndez-López [a,b,*], Nicasio Tomás Jiménez-Morillo [c,d], Felicia Fonseca [e], Tomás de Figueiredo [e], Andrea Parente-Sendín [a,b], Flora Alonso-Vega [a,b], Manuel Arias-Estévez [a,b], Juan Carlos Nóvoa-Muñoz [a,b]

[a] Universidade de Vigo, Departamento de Bioloxía Vexetal e Ciencia do Solo, Área de Edafoloxía e Química Agrícola, Facultade de Ciencias, As Lagoas s/n, 32004 Ourense, Spain
[b] Instituto de Agroecoloxía e Alimentación (IAA), Universidade de Vigo, Campus Auga, Rúa Canella da Costa da Vela 12, 32004 Ourense, Spain
[c] Instituto de Recursos Naturales y Agrobiología de Sevilla (IRNAS-CSIC), Avda. Reina Mercedes 10, 41012 Sevilla, Spain
[d] Instituto Mediterrâneo para a Agricultura, Ambiente e Desenvolvimento (MED), University of Évora, Pólo da Mitra Apartado 94, 7006-554 Évora, Portugal
[e] Centro de Investigação de Montanha (CIMO), Instituto Politécnico de Bragança, Campus de Sta. Apolónia, 5300-253 Bragança, Portugal

HIGHLIGHTS

- The prescribed fire resulted in Hg losses from the uppermost soil layers.
- Mineral soil layers are long-term reservoirs of Hg despite the prescribed fire.
- The well-decomposed SOM leads to higher Hg levels in the finest soil aggregates.
- The easy mobilization of Hg-enriched aggregates into water bodies is of concern.
- Soil Hg before and after the prescribed fire was linked to specific families of SOM.

GRAPHICAL ABSTRACT

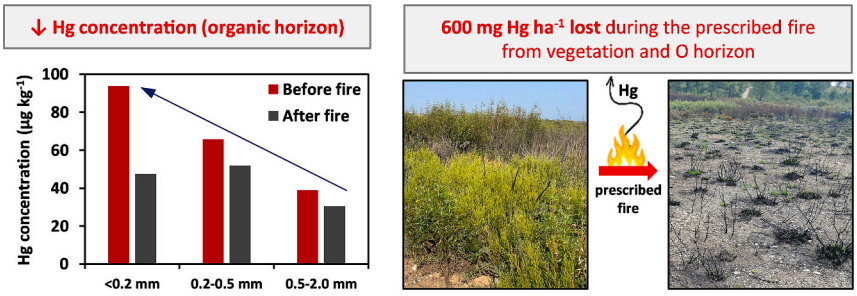

ARTICLE INFO

Editor: Manuel Esteban Lucas-Borja

Keywords:
Hg
Prescribed burning
Re-emission
ATR-FT/IR
Chemometrics
SOM

ABSTRACT

Soils constitute the major reservoir of mercury (Hg) in terrestrial ecosystems, whose stability may be threatened by wildfires. This research attempts to look at the effect of prescribed fire on the presence of Hg in a shrubland ecosystem from NE Portugal, delving into its relationship with soil aggregate size and the molecular composition of soil organic matter (SOM). During the prescribed fire, on average 347 mg Hg ha^{-1} were lost from the burnt aboveground biomass of shrubs and 263 mg Hg ha^{-1} from the combustion of the soil organic horizon. Overall, Hg concentration and pools in the mineral soil did not show significant changes due to burning, which highlights their role as long-term Hg reservoirs. The higher Hg concentrations found in smaller aggregates (<0.2 mm) compared to coarser ones (0.5–2 mm) are favored by the higher degree of organic matter decomposition (low C/N ratio), rather than by greater total organic C contents. The Hg-enriched finest fraction of soil (<0.2 mm) could be more prone to be mobilized by erosion, whose potential arrival to water bodies increases the environmental concern for the Hg present in fire-affected soils. The SOM quality (molecular composition) and the main organic families, analyzed by Fourier-transform infrared spectroscopy in combination with multivariate statistical

* Corresponding author at: Universidade de Vigo, Departamento de Bioloxía Vexetal e Ciencia do Solo, Área de Edafoloxía e Química Agrícola, Facultade de Ciencias, As Lagoas s/n, 32004 Ourense, Spain.
E-mail address: memendez@uvigo.gal (M. Méndez-López).

https://doi.org/10.1016/j.scitotenv.2023.167532
Received 11 July 2023; Received in revised form 22 September 2023; Accepted 30 September 2023
Available online 4 October 2023

analysis, significantly conditioned the retention/emission of Hg in the uppermost soil layers. Thus, before the fire, Hg was strongly linked to lipid and protein fractions, while Hg appeared to be linked to aromatic-like compounds in fire-affected SOM.

1. Introduction

Mercury is recognized as a pollutant of environmental and public health concern worldwide (Clarkson and Magos, 2006), being soil its largest reservoir in terrestrial environments (Grigal, 2003). Mercury distribution through the soil profile is highly heterogeneous. Generally, the upper organic horizon shows the greatest Hg concentration, whose accumulation is favored by its high affinity for soil organic matter (SOM; Meili, 1991; Grigal, 2003; Skyllberg, 2010). Among the diverse chemical components of SOM, thiols are recognized as the preferred functional group for Hg binding (Skyllberg et al., 2003; Ravichandran, 2004). Organic horizons of forest soils usually behave as a source of Hg to the uppermost layers of the mineral soil, where Hg concentration usually decreases with increasing soil depth (Obrist et al., 2012; Navrátil et al., 2016; Gruba et al., 2019). Although the mineral soil tends to show lower Hg concentrations than the organic horizon, the Hg accumulated in deep mineral soil layers is protected against the effect of external disturbances, acting as stable and long-lasting Hg reservoirs (Obrist et al., 2014). Contrarily, the upper organic horizons are highly vulnerable to external changes (i.e. global warming, land use change and forest harvesting) that affect Hg and organic matter dynamics, by either enhancing or worsening their ability to accumulate Hg (Mazur et al., 2014; Wang et al., 2019a, 2019b; Li et al., 2022).

Wildfires constitute a serious environmental problem that causes direct and indirect damage to terrestrial ecosystems. Prescribed fires, commonly of low to moderate severity, are widely used to reduce the effects of the projected increase in wildfire frequency and severity due to global warming, land abandonment and afforestation with flammable species (IPCC, 2013; Moreira et al., 2011). However, there is evidence that both wildfires and prescribed burnings can release Hg from the combustion of vegetation and surface soil (Engle et al., 2006; Biswas et al., 2007; Melendez-Perez et al., 2014; Kolka et al., 2017). Once released into the atmosphere, Hg can suffer long-range transport (Sigler et al., 2003) or local deposition near the wildfire (Witt et al., 2009; Jensen et al., 2017). Hg emissions due to wildfires are expected to increase by almost 30 % by 2050 (Kumar et al., 2018). Post-fire effects were also observed in field experiments, such as the mobilization of Hg-containing surface ash and soil particles through erosion at local scales. Such particles may be mobilized towards aquatic ecosystems, where biogeochemical conditions are favorable for Hg transformation into methyl-Hg, which is more toxic and bioaccumulative (Jensen et al., 2017; Abraham et al., 2018).

Soils affected by wildfires are expected to show a considerable drop in SOM content, particularly in the upper centimeters (Badía-Villas et al., 2014; Girona-García et al., 2018a). However, several authors reported inputs of organic matter from the deposition of the burnt overlying vegetation on the forest floor (Johnson and Curtis, 2001; González-Pérez et al., 2004; Knicker et al., 2005). The migration of fine charred plant debris (<2 mm) from the litter layer to the underlying mineral soil results in increased C concentrations (González-Pérez et al., 2004; Knicker et al., 2005; Jiménez-Morillo et al., 2016). Wildfire-induced changes are not limited to the content but to the quality of SOM. The exposition of SOM to thermal treatments resulted in lower solubility and available functional groups (Almendros et al., 1990; Jiménez-Morillo et al., 2018), which in turn affects its capacity to adsorb and retain nutrients and trace elements (i.e., Hg). Given the well-known relationship existing between Hg and SOM, and particularly with thiol functional groups (Meili, 1991; Skyllberg, 2010), fire-induced changes in SOM are commonly accompanied by variations in Hg dynamics (Grigal, 2003). However, little is known about the impact of SOM quality (molecular composition) alteration on Hg distribution among different particle size fractions. The molecular alteration of SOM by fire was reported to be significantly driven by the particle size fraction of soil (Jiménez-Morillo et al., 2018, 2020, 2022). Some researchers have reported that smaller particle size fractions of soil contain greater Hg concentrations than coarser particles (Grigal, 2003; Béliveau et al., 2009; Burke et al., 2010; Qin et al., 2014; Gómez-Armesto et al., 2020). Moreover, the finest particles are responsible for most of the Hg-containing sediment transport to watersheds (Zheng et al., 2016), where serious toxicity risks are favored. Burke et al. (2010) emphasized the need for further study on the effect of fire on Hg dynamics within different soil particle size fractions as a function of fire-induced changes to SOM.

Against this background, we hypothesized that prescribed fires, although less severe than wildfires, may disturb Hg cycling in the ecosystem. It was also hypothesized that fire-induced changes in the presence of Hg in the soil might depend on the variations in SOM dynamics. Hence, the present study aims to assess changes in SOM and Hg concentrations and pools induced by a prescribed fire performed for forest management purposes in a shrubland in NE Portugal. The effect of the controlled burning on such parameters was evaluated in the organic horizon and at different depths of the mineral soil (up to 20 cm), making a more detailed description in the first 10 cm, being the most influenced by the high temperatures reached during burning. In addition, as initial exploratory research, the study tried to establish links between the concentration of Hg and the composition of SOM in different aggregate size fractions from the uppermost soil layers before and after burning. This is an attempt to understand whether the distribution of Hg in the upper soil layers after fire is linked to the molecular alteration of SOM, and to which biogenic family Hg is preferentially associated with.

2. Material and methods

2.1. Study area

The study was conducted in a shrubland area that was subjected to a prescribed burn to protect a coniferous forest whose extent has been considerably reduced in the past due to several wildfires. The study area belongs to the Montesinho Natural Park, which spreads over a 750 km^2 surface in NE Portugal and whose management plan includes prescribed fire to control shrub expansion in degraded areas. The burnt area was predominantly covered by species typical of shrubland communities of Mediterranean climates, such as *Cistus* sp., *Genista* sp., *Erica* sp. and *Lavandula* sp. The study area (41°54′0" N, 6°40′52.6" W) is 800 m a.s.l., with mean annual temperature and rainfall of 12 °C and 800–1000 mm, respectively, which give rise to a temperate climate with extreme summer heat and drought conditions. The geomorphology of the area is characterized by a plateau incised by deep valleys where small streams flow. The dominant rock type of the area is schist, which is covered by shallow and stony soils, mainly Epileptic Umbrisol (Loamic, Eutric) according to IUSS Working Group WRB (2022).

The controlled burning was conducted in March 2021 over 5 ha of shrubland bordering a small group of pine trees (Fig. S1). The temperature reached by flames was monitored with infrared imaging technology and fire severity was classified as low to moderate (Parsons et al., 2010). Moreover, the first sight after the prescribed fire indicated a large spatial variability in fire severity affecting vegetation or soil to different extents, as also reflected by the different temperatures reported during burning (between 100 and > 670 °C; Fig. S2).

2.2. Sample collection and preparation

In order to estimate Hg losses during the prescribed fire, both vegetation and soil samples (up to 20 cm, $n = 110$) were collected one week before (BF) and one day after (AF) the prescribed fire at 11 fixed locations of the studied area (Fig. S1).

Vegetation sampling was conducted within a 100 × 100 cm area at each of the 11 locations before the prescribed fire. In the square, the whole aboveground biomass was collected distinguishing species of the dominant genus (*Genista*, *Erica* and *Cistus*), which described an interleaved distribution through the study area. The quantification of the total aboveground biomass by species per surface area was made by on-site weighing, from which a representative aliquot of each species at each location has been taken to the laboratory for Hg analysis. Immediately after the prescribed fire, the remaining biomass was estimated by field observations establishing combustion factors for each dominant species (Fonseca et al., 2022).

Soil sampling was done by differentiating the organic horizon from the mineral soil. Organic horizon samples were collected in duplicate (before and after the prescribed fire) at the 11 fixed locations ($n = 22$) within a square area of 70 × 70 cm, taking into account their thickness to later determine the bulk density as a function of the total dry mass of soil collected. At the same 11 locations, mineral soil samples were also collected before and after fire and at different depth intervals: 0–3, 3–6, 6–10, 10–20 cm ($n = 88$). At each interval, a soil core (100 cm^3) was carefully collected for bulk density estimation, corrected considering dry mass at the constant weight (105 °C). In addition, samples of fresh parent rock (schist and quartz) were collected to evaluate baseline geogenic Hg levels.

Sample preparation before chemical analyses started with the oven-drying of vegetation (separated by species) and soil (organic and mineral) samples at 40 °C. After drying, vegetation and organic horizon samples were weighed and ground to <4 mm, whereas mineral soil samples were sieved to <2 mm. An aliquot of each sieved/ground sample of vegetation and soil was powdered in an automated agate mortar for subsequent analyses.

The organic horizon and the upper mineral soil layer would experience the highest temperatures during burning and would likely undergo the greatest variations in Hg and SOM. Therefore, samples of the organic horizon and mineral topsoil (0–3 cm) from two representative locations of the study area (2 and 10) before and after the prescribed fire ($n = 8$) were selected for further analyses. Before analyses, an aliquot of the fine earth fraction (<2 mm) of the selected samples was separated and the rest of the sample was sieved by physical methods (stainless steel sieves) to different size intervals: <0.2 mm, 0.2–0.5 mm, and 0.5–2 mm, which were weighed and powdered, resulting in 24 soil samples of different size. These samples were analyzed to determine the concentration of total Hg, total C, total N and identify the composition of soil organic matter (SOM) by Fourier Transform-Infrared Spectroscopy (FT-IR). All equipment used during sample preparation was cleaned with diluted acid and deionized water to minimize cross-contamination.

2.3. Chemical analyses and calculations

For the analysis of Hg concentration in powdered vegetation and soil samples, a Milestone tri-cell Direct Mercury Analyzer (DMA-80) was used by applying thermal decomposition, amalgamation and atomic absorption spectroscopy (EPA Method 7473). Total Hg concentration was measured in two replicates of each sample and the average concentration was calculated. Additional replicates were analyzed if the coefficient of variation (CV) was above 10 %. For quality assurance and control (QA/QC), several standard reference materials (SRM) were analyzed, obtaining percent recoveries of 106 and 116 % for BCR 142 R (sandy soil, Hg certified at 67 ± 11 μg kg^{-1}) and NIST 1547 (peach leaves, Hg certified at 31 ± 7 μg kg^{-1}), respectively.

Total concentrations of organic carbon (C) and nitrogen (N) of the powdered soil samples were analyzed using a Thermo-Finnigan 1112 Series NC elemental analyzer and using the SRM NCS 33840026 for QA/QC purposes.

The concentration of total Hg ($Hg_{conc.}$), the bulk density (BD), and the thickness (THI) of the organic horizons and mineral soil layers at different depth intervals were used to calculate the Hg pool (Hg_{pool}) before (BF) and after (AF) the prescribed fire by applying Eq. (1). The same procedure was followed to calculate C pools, but taking into account the C concentration.

$$Hg_{pool} = Hg_{conc.} \text{ x BD x THI} \quad (1)$$

The Hg pool BF in the main shrub species present in the study area was estimated considering the Hg concentration and dry mass of each species per surface area. The Hg pool in vegetation AF was estimated by applying the combustion factor to the Hg pool determined for each species BF. Therefore, we assumed that all the Hg present in vegetation BF was lost together with the burnt biomass, either being deposited as ash on the soil surface or being volatilized to air. The loss of Hg from vegetation and soils during burning was estimated as the difference between the corresponding Hg pools BF and immediately AF.

The molecular composition of different size fractions of bulk soil samples was measured by Fourier Transform-Infrared Spectroscopy (FT-IR) technique (Coradeschi et al., 2023). Fourier Transform Mid-Infrared spectra were obtained using an Alpha-R™ Spectrometer (Bruker Optics®, Germany), with Attenuated Total Reflectance (ATR) module (Platinum-ATR-sampling module, Bruker, Germany), at a wavelength range of 4000–400 cm^{-1} and a resolution of 2 cm^{-1}. To improve the signal to noise ratio, 60 spectra were co-added and averaged for each recorded spectrum. Spectral data were background corrected to a reference spectrum obtained before every measurement, and some spurious absorptions, such as peaks from atmospheric CO_2, could be removed.

2.4. Statistical analyses

Statistical verifications were made using IBM SPSS Statistics 25. The effect of the prescribed fire and different soil layers on Hg concentration and pools and some parameters related to soil organic matter was assessed by applying the non-parametrical Mann-Whitney (*U*) tests. The data were tested with Spearman's rank test (r_s) to look for the statistical significance of correlations between the variables studied. These statistical tests were performed by differentiating organic and mineral soil layers, different particle size intervals and the situation relative to the prescribed burning (before or after fire). Statistical significance was considered when $p < 0.05$, unless otherwise specified.

Partial Least Squares (PLS) regression models were generated using the ParLeS software (Viscarra Rossel, 2008) and employed to acquire predictive models of Hg concentration from the FT-IR spectral intensities in the range 4000–800 cm^{-1} (independent variables, 600 data points). The spectral pre-processing treatments consisted of a light scatter and baseline correction by Standard Noise Variate (SNV), a denoising by using a median filter, and a mean centering (De la Rosa et al., 2019; Jiménez-González et al., 2019; Coradeschi et al., 2023). The Root Mean Squared Error (RMSE) and the Akaike's Information Criterion (AIC) were used, to prevent overfitting and to determine the best number of factors (latent variables) for each model. Lastly, the diagnostic spectral regions of the FT-IR spectra were studied by the combination plot of the Variable Importance for Projection (VIP) values in the studied spectral range. The VIP traces can be useful to identify the independent variables (spectral peaks), that may be linked to the dependent variable (Hg concentration). Spurious forecast models due to overfitting were discarded after comparing PLS models calculated with the randomized data of Hg concentration (dependent variable).

3. Results

3.1. Fire-induced changes in plant and soil Hg concentrations and pools

Pre-fire (BF) and after fire (AF) averages of Hg concentration and Hg pools in the aboveground biomass of the dominant shrub species in the study area are summarized in Table 1. The total Hg concentration varied between 10.3 and 27.0 μg kg^{-1}, with the highest mean values observed in individuals of the genus *Erica*. Regarding the pool of Hg in the aboveground plant biomass, the values were in the ranges 32–425 mg ha^{-1} and 7–85 mg ha^{-1} before and after the prescribed fire, respectively, with *Erica* sp. showing the highest mean Hg pool (Table 1).

The mean concentration and pool of Hg in soils before and after the prescribed fire are depicted in Fig. 1. In general terms and under undisturbed conditions (i.e. before the prescribed fire), the mean concentration of total Hg was lower in the organic horizon (53 μg kg^{-1}) than in the underlying mineral soil layers (54–68 μg kg^{-1}), although without significant differences ($p > 0.05$). In the mineral soil layers, the concentration of Hg slightly decreased with soil depth (Fig. 1), resulting in a reduction of 19 % in the deepest layer (10–20 cm) compared to the value observed in the 0–3 cm layer. Regarding the pool of Hg, the mean value of the organic horizon before the prescribed fire was 0.04 mg m^{-2}, two orders of magnitude lower than the range of values found in the mineral soil layers (1.5–5.4 mg m^{-2}), where the Hg pool increased with soil depth. This resulted in significant differences among the pool of Hg in the organic layer compared to the mineral soil before the fire ($U = 25.929$; $p = 0.000$; $n = 55$). Contrarily to Hg concentration, the pool of Hg in the mineral soil layers increased with soil depth (Fig. 1).

The prescribed fire resulted, on average, in a reduction of total Hg concentration in the organic (O) horizon (from 53 to 42 μg kg^{-1} BF and AF, respectively; Fig. 1), being significantly lower than that observed before burning ($U = 26.000$; $p < 0.05$; $n = 22$). The reduction of total Hg in the O-horizon occurred in 9 of the 11 locations, being highly variable (3–70 %), while in the other two locations, Hg concentration increased considerably after burning (53 and 132 %) (Fig. S3).

In the mineral soil layers, Hg concentration did not vary significantly ($p > 0.05$) before and after the prescribed burning. The mean concentration of Hg in the soil layer immediately underlying the organic horizon, i.e. 0–3 cm, decreased after burning from 68 to 64 μg kg^{-1} (Fig. 1). However, the effect of fire on Hg concentrations at the 0–3 cm layer was highly variable among locations, resulting in Hg losses or enrichments up to 49 and 59 %, respectively. In the 3–6 cm and 6–10 cm soil layers, the prescribed fire resulted in a mean Hg loss of <2 %, although showing high variability in Hg concentrations among the 11 locations (Fig. S3). In the deepest mineral soil layer (10–20 cm) there was also variability in Hg concentrations before and after fire although, contrarily to the overlying layers, the mean Hg concentration showed a slight increase after burning (5 %).

Regarding the pool of Hg in the organic horizon, a considerable but not significant ($p > 0.05$) reduction was observed in its mean value after the fire, declining from 0.04 to 0.02 mg m^{-2} (Fig. 1), which represents on average a 59 % Hg loss. In further detail, 8 of the 11 locations showed a considerable drop (31–90 %) in the Hg pool (Fig. S4). Contrarily, the organic horizon in the other 3 locations showed notable increases in Hg pools, two of them coinciding with those that showed rising Hg concentrations after burning.

Mercury pools in the mineral layers were slightly higher after the prescribed fire (Fig. 1), although without statistical significance ($p > 0.05$). Thus, percent increases in the Hg pool varied between 7 and 15 % in the 6–10 cm and 3–6 cm soil layers, respectively. Like Hg concentration, there was great variability in Hg pool changes induced by fire in the mineral soil among locations (Fig. S4).

Table 1
Average and standard deviation of Hg concentration and pools in the aboveground biomass of three dominant shrub species before (BF) and after (AF) the prescribed fire.

Species	N	Hg conc. BF	Hg pool BF	Hg pool AF
		μg kg^{-1}	mg ha^{-1}	
Cistus sp.	5	16.0 ± 5.1	53 ± 24	26 ± 12
Genista sp.	11	16.6 ± 2.8	182 ± 122	36 ± 24
Erica sp.	6	24.7 ± 2.3	220 ± 141	44 ± 28

3.2. Fire-induced changes related to SOM

Due to the close relationships between Hg and organic C cycles in terrestrial ecosystems (Skyllberg, 2010; Smith-Downey et al., 2010), changes in Hg concentrations and pools due to prescribed fire effects are expected to be linked, in part, to variations in soil organic matter (SOM). Therefore, the results obtained for some parameters related to SOM before (BF) and after (AF) the prescribed fire are described in this section (Fig. 2; Table S1).

Before the prescribed fire, total organic C (TOC) concentration in the organic horizon was on average 5–8 times greater than in the mineral soil, where TOC decreased with depth from 84 g kg^{-1} (0–3 cm) to 50 g kg^{-1} (10–20 cm) (Fig. 2). The mean concentration of total N ranged from 2.7 to 11.6 g kg^{-1}, showing greater values in the O-horizon and decreasing with mineral soil depth (Fig. 2). The highest mean C/N ratio occurred in the organic horizon (38), varying between 19 and 21 in the mineral soil (Fig. 2). The mean C pool was higher in the mineral soil layers (2.4–2.8 kg m^{-2}) than in the organic horizon (0.3 kg m^{-2}).

After the prescribed fire, TOC was reduced by about 7 % in the organic horizon (at 7 locations) and in the 0–3 cm layer (at 6 locations), with a low reduction (<3 g kg^{-1}) below 3 cm depth (Fig. 2). Mean values of total N increased slightly after the fire (5–8 %) at all depths, except in the 0–3 cm layer where it was reduced by 2 %. A slight decrease in the C/N ratio was observed for all soil layers after the prescribed fire, being more evident in the organic horizon (14 %) than in the mineral soil (3–7 %). The C/N ratio before and after the prescribed fire was significantly different in the O-horizon ($U = 21.000$; $p < 0.01$; $n = 22$) and in the 0–3 cm layer ($U = 26.000$; $p < 0.05$; $n = 22$). Regarding the C pool, there was a considerable reduction in the organic horizon (46 %) after burning, while it increased slightly (2–3 %) in the 3–6 and 6–10 cm layers, and strongly (31 %) in the 10–20 cm layer.

3.3. Fire-induced changes in Hg and SOM in different size fractions

Before the prescribed fire, higher Hg concentrations were found in the smaller aggregate size fractions (hereinafter referred to as fractions) from both the organic horizon and the 0–3 cm mineral layer (Table 2). Thus, mean values of Hg concentration followed the sequence: 94 μg kg^{-1} (<0.2 mm) > 66 μg kg^{-1} (0.2–0.5 mm) > 39 μg kg^{-1} (0.5–2 mm) in the organic horizon and 85 μg kg^{-1} (<0.2 mm) > 70 μg kg^{-1} (0.2–0.5 mm) > 36 μg kg^{-1} (0.5–2 mm) in the 0–3 cm mineral layer. The concentration of total C (66–468 g kg^{-1}) and the C/N ratio (21–46) increased with greater aggregate size, showing higher values in the organic horizon than in the 0–3 cm mineral layer. The concentration of total N ranged from 2.7 to 12.7 g kg^{-1}, showing higher values in the organic horizon than in the 0–3 cm layer (Table 2).

After the prescribed fire there was a reduction of Hg concentrations in the different fractions of the organic horizon, showing Hg losses of 49 % (<0.2 mm), 21 % (0.2–0.5 mm) and 22 % (0.5–2 mm). In contrast, the concentration of Hg in the 0–3 cm mineral layer increased in <0.2 mm, 0.2–0.5 mm, and 0.5–2 mm fractions at 3, 7 and 26 %, respectively. TOC and the C/N ratio described the same trend as for Hg concentration, showing a considerable loss in the organic horizon and a slight increase in the 0–3 cm layer after burning (Table 2). Total N concentration did not suffer notable variations after burning, except in the <0.2 mm fraction of the O-horizon (Table 2).

The average IR and 2nd derived spectra of SOM in bulk soil samples (i.e. the fine earth fraction; <2 mm) of the O-horizon and the 0–3 cm

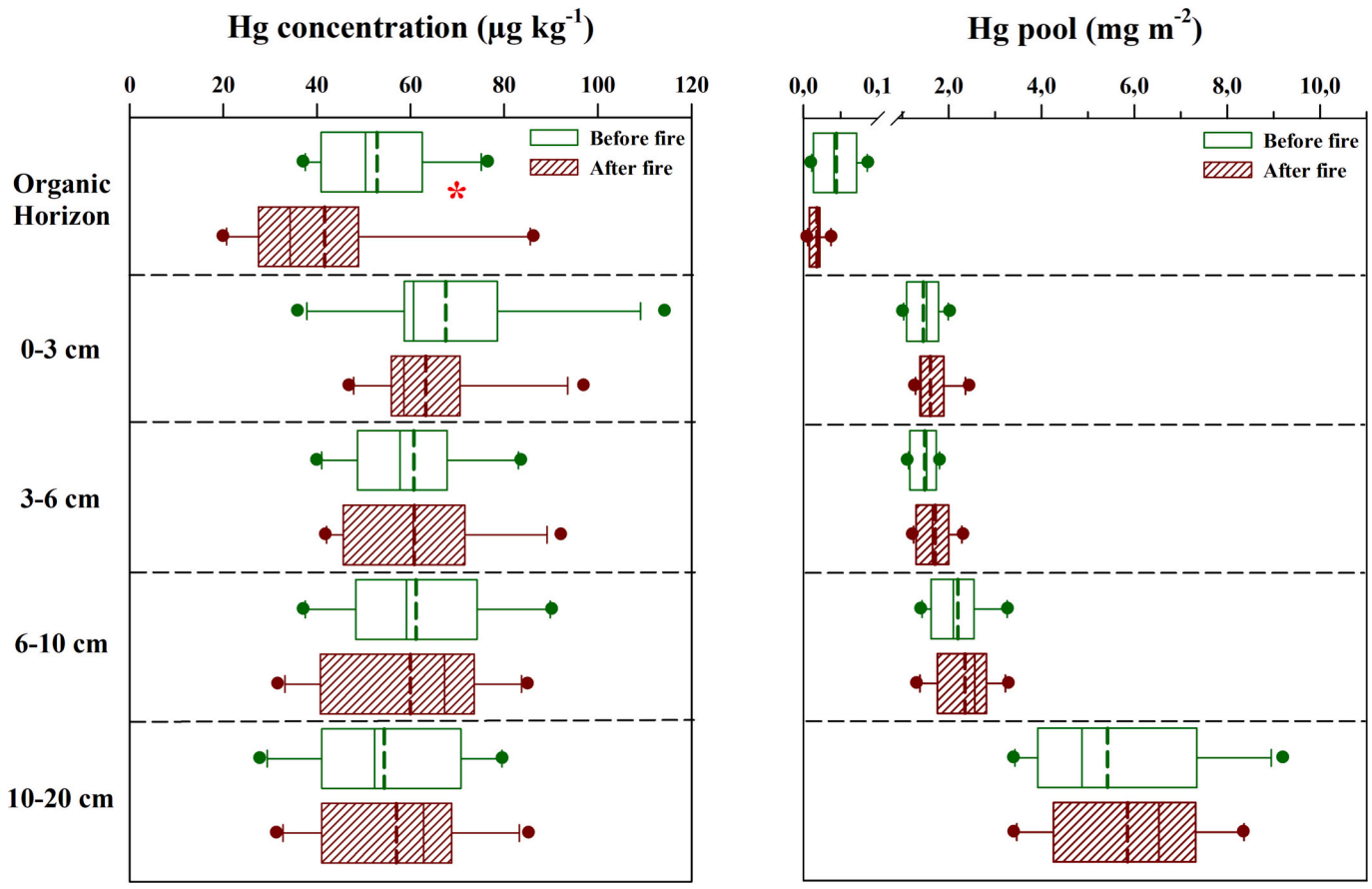

Fig. 1. Box and whisker plot of total Hg concentration and pool in the organic horizon and at different depth intervals of the mineral soil. The box shows the interquartile range (from 25th to 75th percentiles), the solid line in the box represents the median value (50th percentile) and the dashed line represents the average value. The whiskers extend from the minimum to the maximum value. The points outside the box are outliers. * means significant differences before and after the fire ($p < 0.05$) according to the Mann-Whitney test.

depth before (blue) and after (red) the prescribed fire (Fig. 3) exhibit some differences. The bulk soil samples are dominated by the band at 1000 cm^{-1}, which corresponds to lignin-derived compounds and some ester and alcohol molecules (McCarthy and Rice, 1985; Miralles et al., 2007). Additional significant bands include those at 520 and 450 cm^{-1}, together with those at 780 and 680 cm^{-1}, which are assigned to quartz and silicates, i.e., the mineral component of soils (Ojima, 2003). The band at 1160 cm^{-1} is connected with hydroxyl groups (Hasan and Masoud, 2014), whereas the band at 1100 cm^{-1} is associated with the deformation of OH groups, specifically the hydroxyl group of methoxyphenols (Miralles et al., 2007; Jiménez-González et al., 2019; Coradeschi et al., 2023). The band at 1640 cm^{-1}, which relates to unspecific aromatic vibrations (Dupuis and Jambu, 1969), was also detected in all samples.

However, there are some differences among unburned and burned samples, as well as among soil layers. Within the O-horizon, there is a remarkable elimination of the band at 2900 cm^{-1} after the prescribed fire. This band corresponds to alkyl compounds (2900–2920 cm^{-1}; Miralles et al., 2007). In addition, there is a removing of the bands located between 1900 and 1300 cm^{-1} (see the 2nd derived spectra, Fig. 3). This cluster of IR bands is associated to amine groups and aromatic compounds (Zhou et al., 2014). Finally, bands around 900 cm^{-1} experimented a noticeable alteration, since in SOM of unburned samples, the first band (960 cm^{-1}) is higher than the second one (910 cm^{-1}), but in burned samples there is change of the band intensity (960 cm^{-1} band is higher than 910 cm^{-1} band). The band at 910 cm^{-1} is assigned to either aromatic or oleophilic C—H out-of-plane deformations (Miralles et al., 2007; Coradeschi et al., 2023), while, C═C bending of alkene corresponds to the band at 960 cm^{-1}. Concerning the 0–3 cm layer, there are not remarkable differences between FT-IR spectra. Only the 2nd derived spectra show a little alteration in the region 1900–1300 cm^{-1}. Concerning molecular differences among soil layers (O-horizon and 0–3 cm depth), the upper soil layer (O-horizon) before fire shows some bands that are not observed in the 0–3 cm layer, such as 2900 cm^{-1}, as well as 1490 cm^{-1} (amide II group; Tarantilis et al., 2012). Observing the 2nd derived spectra of the 0–3 cm layer and O-horizon, the alteration in the relative intensity of bands located between 960 and 910 cm^{-1} is also detected.

We also investigated the molecular composition of organic matter held in different particle size fractions, in the O-horizon (Fig. S5) and in the 0–3 cm layer (Fig. S6). When the fractions analyzed in the O-horizon (Fig. S5) are considered, it is clear that they display similar spectral patterns to the average in bulk soil samples (Fig. 3), as well as equivalent alterations generated by the prescribed fire. However, a significant difference is shown in the finest particle size fraction (<0.2 mm), where a clear spectrum disturbance appears between 1900 cm^{-1} and 1300 cm^{-1}, as well as changes at 960 and 910 cm^{-1}. Surprisingly, the typical band associated with aliphatic chemicals at 2900 cm^{-1} (Miralles et al., 2007) is lacking within this fraction. In contrast, only a modest change in the 1900–1300 cm^{-1} spectral area is found inside the smallest particle size fraction (<0.2 mm) within the aggregate fractions from the soil layer between 0 and 3 cm in depth (Fig. S6).

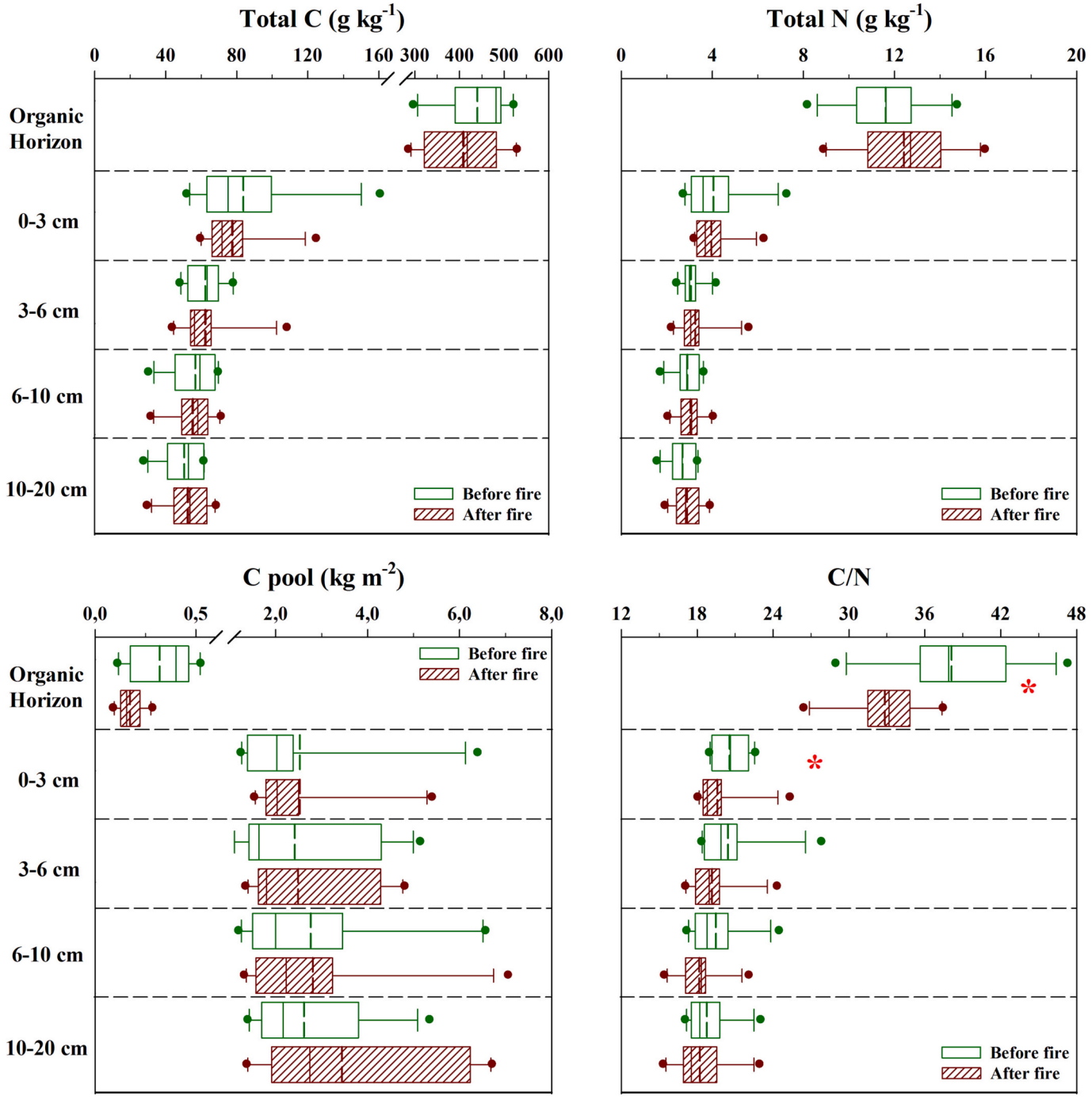

Fig. 2. Box and whisker plots of different parameters related to SOM in the organic horizon and at different depth intervals of the mineral soil. The box shows the interquartile range (from 25th to 75th percentiles), the solid line in the box represents the median value (50th percentile) and the dashed line represents the average value. The whiskers extend from the minimum to the maximum value. The points outside the box are outliers. * means significant differences before and after the fire ($p < 0.05$) according to the Mann-Whitney test.

3.4. FT-IR spectroscopy and PLS analysis of Hg concentration in different soil layers

The cross-validation plots (predicted vs. observed values) for the Hg concentration of unaffected and burned soils at different depth layers (O-horizon and 0–3 cm) are depicted in fig. S7. The PLS models, using exclusively the information contained in a discrete infrared spectra range (4000–800 cm^{-1}, 600 data points), successfully predicted the Hg concentration of soil samples before and after the prescribed fire. To avoid the impact of the mineral fraction of soil samples, the IR-bands between 800 and 400 cm^{-1} have been discarded. Comparison with an alternative model derived from the fully randomized dependent variable (Hg concentration) that had no connection ($p > 0.05$) with infrared data validated the model's accuracy (data not shown). Each of the Hg concentration forecast models generated from the average infrared spectra of soil samples before (O-horizon: $r^2 = 0.994$, $p = 0.0001$; 0–3 cm: $r^2 = 0.904$, $p = 0.0003$) and after (O-horizon: $r^2 = 0.935$, $p = 0.0007$; 0–3 cm depth: $r^2 = 0.924$, $p = 0.0002$) prescribed burning, indicate substantial significance. The RMSE and AIC values in all situations advised that four factors can be used for both scenarios (data not shown).

Table 2
Average and standard deviation of Hg, C and N concentrations and C/N ratio in different fractions of the organic horizon and the 0–3 cm mineral soil layer before (BF) and after (AF) the application of the prescribed fire. Two samples were analyzed for each combination of soil layer, aggregate size and time relative to fire.

Soil layer	<0.2 mm		0.2–0.5 mm		0.5–2 mm	
	BF	AF	BF	AF	BF	AF
			Hg concentration (μg kg^{-1})			
O-horizon	94 ± 6	47 ± 17	66 ± 14	52 ± 11	39 ± 3	30 ± 8
0–3 cm	85 ± 27	88 ± 40	70 ± 15	75 ± 35	36 ± 2	46 ± 26
			C concentration (g kg^{-1})			
O-horizon	343 ± 82	135 ± 17	461 ± 36	263 ± 12	468 ± 41	296 ± 16
0–3 cm	90 ± 12	96 ± 39	123 ± 5	128 ± 52	66 ± 8	77 ± 34
			N concentration (g kg^{-1})			
O-horizon	12.7 ± 3.8	6.5 ± 0.2	12.7 ± 2.7	10.9 ± 1.2	10.3 ± 2.1	10.3 ± 0.8
0–3 cm	4.3 ± 0.1	4.4 ± 1.3	5.0 ± 0.3	5.0 ± 1.8	2.7 ± 0.3	3.0 ± 1.3
			C/N ratio			
O-horizon	27 ± 2	21 ± 2	37 ± 5	24 ± 1	46 ± 5	29 ± 1
0–3 cm	21 ± 2	21 ± 3	25 ± 1	25 ± 1	25 ± 1	25 ± 0

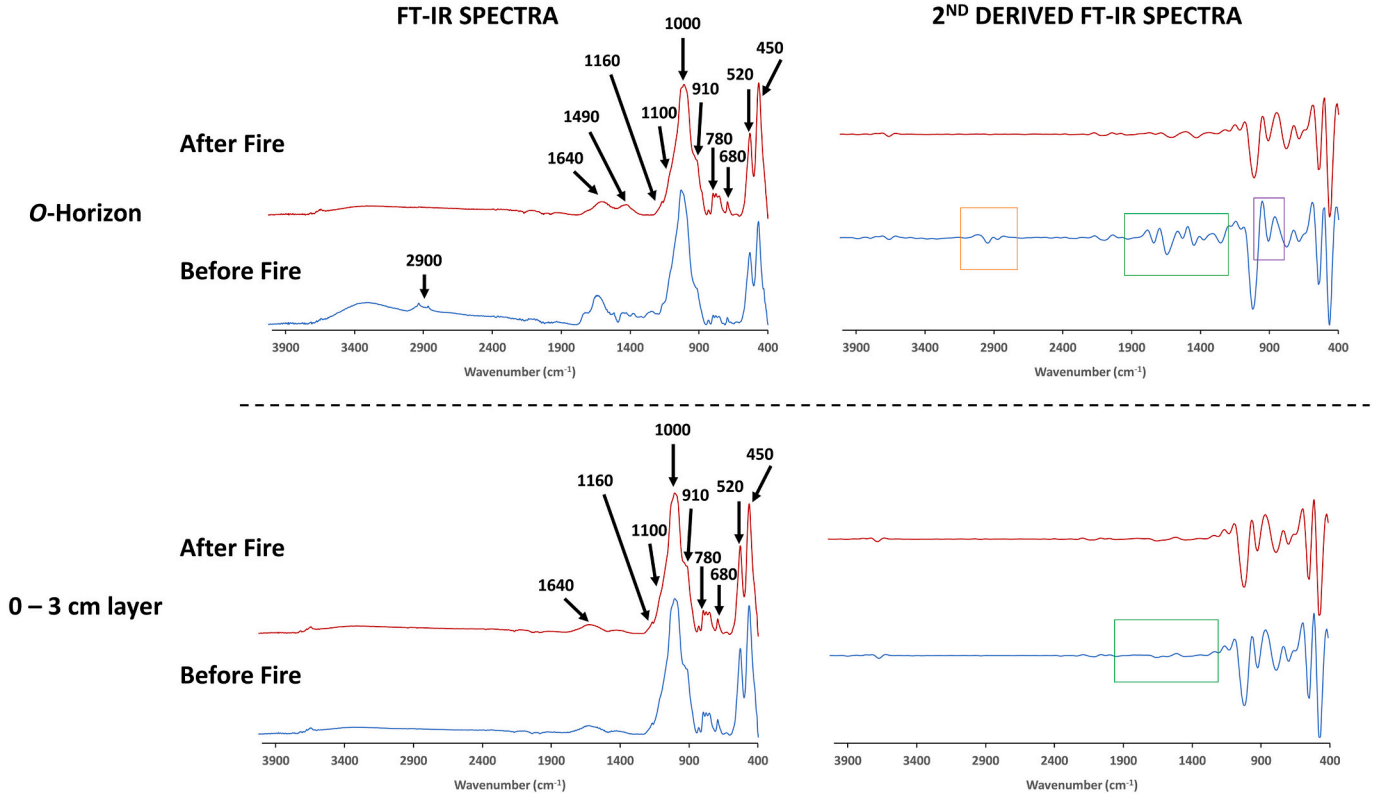

Fig. 3. Average FT-IR spectra (4000–400 cm^{-1}) and 2nd derived spectra (4000–400 cm^{-1}) of SOM in bulk soil samples (i.e., fine earth fraction, <2 mm) of the O-horizon and 0–3 cm depth before (blue) and after (red) the prescribed fire. The colored squares in 2nd derived spectra are indicative of the remarkable molecular changes.

Fig. 4 shows the VIP values of FT-IR spectra for the unburned and burned SOM preserved in the O-horizon and 0–3 cm depth layer, which was used to obtain the different PLS models. The superposition of the average infrared spectrum of SOM with the VIP trace indicates the best diagnostic bands to predict the Hg concentration for each scenario. The most significant FT-IR bands to predict the Hg concentration for unaffected and fire-affected SOM in the O-horizon are those positioned at 2900, 1640, 1490, 1160 and 1000, and 1640, 1100 and 910 cm^{-1}, respectively. In contrast, for the 0–3 cm depth, the unburned SOM infrared spectrum is dominated by the bands at 1490, 1100, 1000 and 910 cm^{-1}, while bands at 1100 and 910 cm^{-1} are the most important ones in burned organic matter within 0–3 cm soil depth. The VIPs observed between 2300 and 1800 cm^{-1} were not considered in the model generation because they are associated with the presence of CO_2, just as the VIPs observed between 4000 and 3000 cm^{-1} are associated with the presence of H_2O molecules in the sample.

The models developed to forecast Hg concentration in various circumstances regarding burning and different depths were validated by

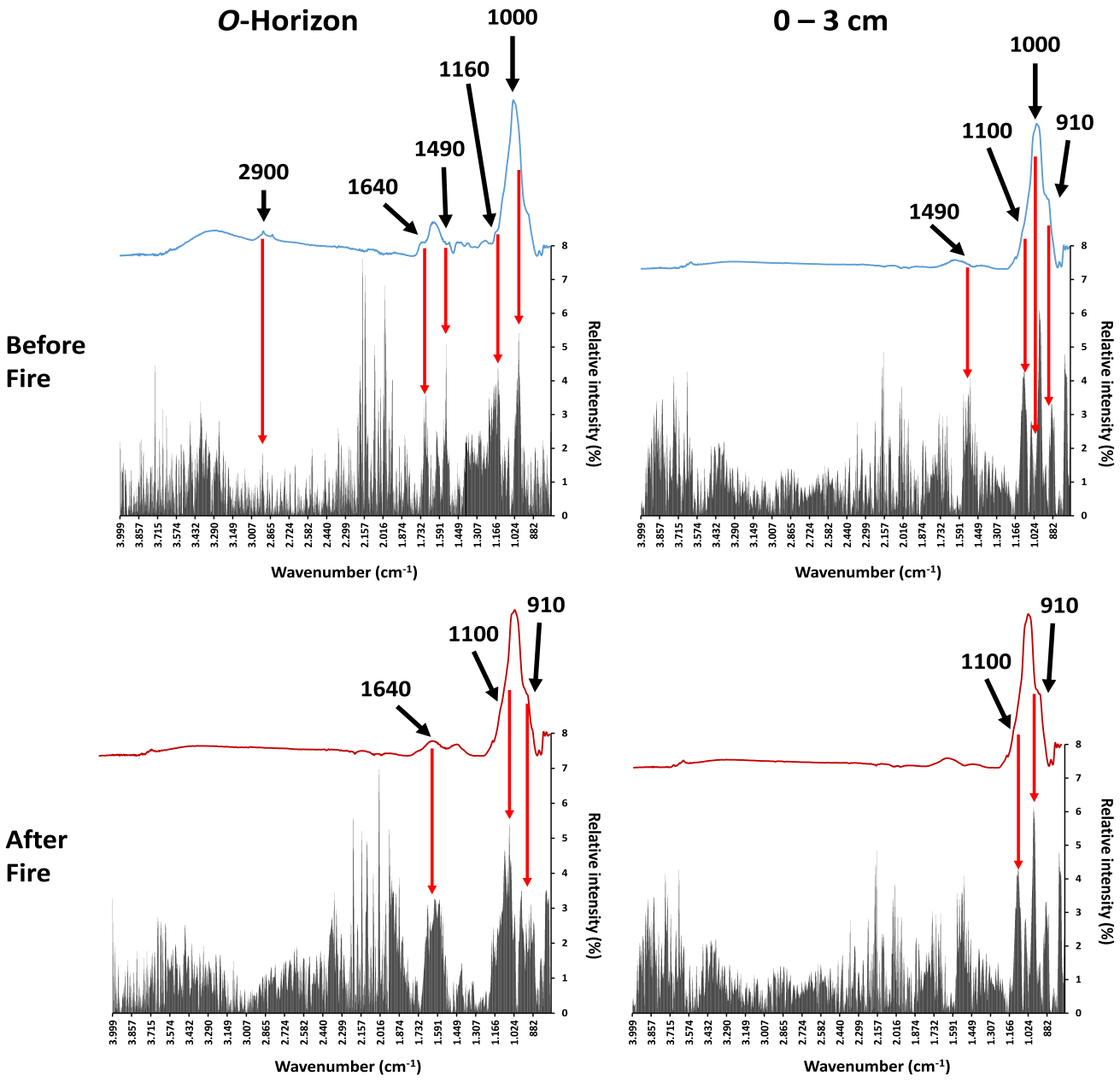

Fig. 4. Superposition of Variable Importance for Projection (VIP) of spectral points and average infrared spectra of SOM from O-horizon and 0–3 cm depth layer before (blue) and after (red) the prescribed fire.

adding the infrared spectra of bulk soil samples (<2 mm) to the forecasting models and comparing the predicted findings with those obtained by elemental analysis (Fig. 5). In all cases, the predicted Hg concentration values did not differ significantly from the observed values, with the exception of the organic matter preserved in the fire-affected O-horizon. In this case, the Hg concentration values predicted were significantly higher than the values obtained straight from the analysis. It is also worth noting that the Hg content derived from models of unaffected organic matter, both in the O-horizon and the 0–3 cm layer, were closer to the measured levels (Fig. 5).

4. Discussion

4.1. Fire-induced changes in plant and soil Hg concentrations and pools

The Hg concentration found in the aboveground biomass of scrubs before the fire was in the range (10–40 μg kg^{-1}) reported in shrublands from different regions of the world (Zhou et al., 2021). The total Hg flux lost due to the combustion of the aboveground biomass was 347 mg ha^{-1}, with 26, 145 and 176 mg ha^{-1} corresponding to *Cistus* sp., *Genista* sp. and *Erica* sp., respectively. *Genista* and *Erica* species showed a greater reduction in Hg pools (Table 1) than species of the genus *Cistus,* due to higher combustion factors in the former, as reported Fonseca et al. (2022). Variations in the combustion degree among different species could be related to the variable composition of natural fibers (Dorez et al., 2014). The Hg lost from the burned vegetation would mostly be released to the atmosphere or deposited on the soil associated with burnt plant debris and ash that may still contain Hg despite burning (Homann et al., 2015; Witt et al., 2009).

Under undisturbed conditions, the concentration of Hg in the organic horizon (37–77 μg kg^{-1}) was lower than that reported in O-horizons (65–170 μg kg^{-1}) from coniferous and deciduous forests located close to the study area (Méndez-López et al., 2022). In the mineral soil, total Hg concentration was 2–3 times greater than the mean (10–20 μg kg^{-1})

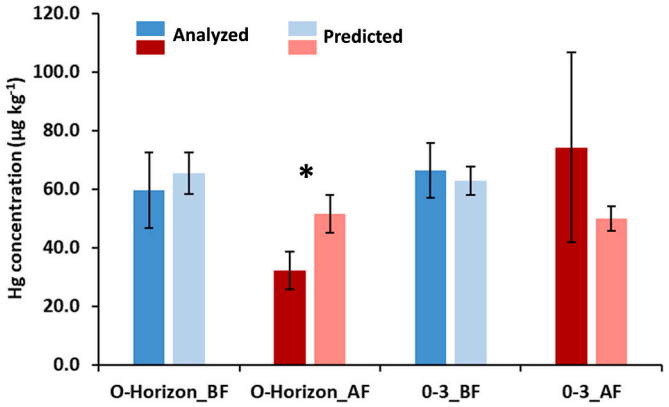

Fig. 5. Comparison of analyzed Hg concentration vs. predicted Hg concentrations in different layers (O-horizon and 0–3 cm) between before (BF) and after (AF) fire from the forecasting FT-IR models. * indicates significant differences ($p < 0.05$).

reported by Olson et al. (2022) in shrublands from the North American deserts. The extreme climatic conditions in this region of the US could result in reduced biomass growth by the dominant shrub species, originating SOM-poor sandy soils that would not favor Hg retention in the mineral layers. The progressive diminution of Hg concentration and TOC with depth, typical of forest soils (Obrist et al., 2012; Navrátil et al., 2014, 2016; Gruba et al., 2019; Vieira et al., 2022), points out the strong affinity between them (Meili, 1991; Grigal, 2003; Skyllberg, 2010), which were positively correlated in the mineral soil ($r_s = 0.598$; $p = 0.000$; $n = 44$; Fig. 6). The low Hg concentration in the parent material (2–4 µg kg^{-1}) excludes a significant contribution of geogenic sources to Hg present in the mineral soil.

The effect of wildfires on Hg pools in terrestrial ecosystems is highly dependent on fire severity (Biswas et al., 2007; Kolka et al., 2017), being prescribed fires an example of low to moderate fire severity. In the present study, the significant ($p < 0.05$) reduction in soil Hg concentration in the organic horizons after burning evidences that the application of prescribed fires of low severity can produce considerable Hg losses, as previously reported (Obrist et al., 2009; Melendez-Perez et al., 2014; Kolka et al., 2017; Abraham et al., 2018). Thus, the organic horizon lost 21 % of its total Hg concentration, comparable to the 27 % total Hg removal reported after a prescribed fire applied to bushy vegetation in Australia (Abraham et al., 2018). Variable Hg losses from organic horizons could result from the combined effect of several factors related to fire (severity, intensity), environmental conditions (humidity, wind speed, air temperature) and vegetation and soil (horizon thickness, pre-fire Hg levels, species and fuel load) (Biswas et al., 2007, 2008; Homann et al., 2015). These factors were reported to vary in very short distances influencing the effect of prescribed fires (Alcañiz et al., 2018). In the present study, some locations showed total Hg concentration increases in the uppermost soil layers after the prescribed fire (Fig. S3). For instance, at location 11, the increase of Hg concentration in the organic horizon was accompanied by a decline in total Hg (up to 50 %) in the underlying mineral soil layer (0–3 cm). In this case, the Hg lost from the 0–3 cm layer could be volatilized and trapped by charred organic matter in the O-horizon. At location 6, the increase of total Hg concentration in the O-horizon and in the underlying 0–3 cm layer (Fig. S3) after burning can be justified by a lower effect of fire at this sampling site and by the deposition of partially burned plant debris containing Hg, which agrees with the increase in total C (23 %) observed at that location (Table S2).

The prescribed fire resulted in <5 % Hg loss in the mineral soil, and the lack of significant differences between Hg concentrations BF and AF (Fig. 1) suggests a scarce effect of fire at those depths. In fact, the temperature reported at 2 cm below the mineral soil surface during a prescribed fire in shrubland from NW Spain (Fernández et al., 2008) was well below that required for Hg volatilization (above 100 °C, Biester and Scholz, 1997). The increase in Hg concentration after fire at the 0–3 cm mineral layer in some locations (Fig. S3) could result from the mobilization of ash towards the mineral soil (Campos et al., 2015), which were recognized as effective Hg adsorbents (Burke et al., 2010). Accordingly, we can hypothesize that the total Hg increase observed in all the mineral soil layers at locations 3 and 10 (Fig. S3) may be due to its mobilization with ash up to 20 cm depth, which would be supported by the increase in total C after burning in the mineral soil at these locations (Table S2). However, the short time elapsed between the fire and the collection of burned samples reduces the consistency in the mobilization of ash-associated Hg down to 20 cm depth. Another possibility is that the spatial variation could explain the differences observed in Hg concentrations before and after fire at different depths among the 11 locations.

Before fire, the considerably lower Hg pool in organic horizons than in mineral layers is consistent with the reduced bulk density, thickness (0.9–1.9 cm) and Hg concentrations in the former (Fig. 1, Table S1), a relationship that has been reported in other studies (Obrist et al., 2012; Gruba et al., 2019). The spatial variability observed in Hg pools among the 11 locations after the prescribed fire could result from fire-induced changes in Hg concentrations and soil bulk density. On one hand, the overall reduction in soil Hg pools after fire at most locations (Fig. S4) would be mostly due to the decreased Hg concentration after fire, which was accompanied by a generalized reduction in total C concentrations AF (Fig. 2). On the other hand, raising Hg pools in mineral layers at locations 3 and 10 AF (Fig. S4) would be favored not only by the increase in total Hg and C concentrations due to fire, but to the increase in bulk density at these locations AF. Contrarily, Hg pool in mineral soil layers at location 7 (Fig. S4) showed little or no change despite the considerable reduction in Hg and C concentrations (Fig. S3; Table S2). These Hg and C losses could be offset by the notable increase in soil bulk density at this location after fire (data not shown), which would help to keep the Hg pools unchanged.

Due to the direct exposition of the O-horizons to fire, differences in the Hg lost between organic and mineral soil layers are expected. In addition, as Hg volatilization is highly dependent on temperature (Biester et al., 2002), less Hg loss is expected in the mineral soil, as temperature during fire declines rapidly with soil depth (Fernández et al., 2008; Mataix-Solera et al., 2011; Melendez-Perez et al., 2014). Therefore, during the prescribed fire in the study area, Hg was mainly lost from the organic horizon and vegetation rather than from the mineral soil. Similar findings were evidenced by Engle et al. (2006), whereas other studies reported small or negligible Hg losses after burning (Biswas et al., 2008; Melendez-Perez et al., 2014; Kolka et al., 2014, 2017; Campos et al., 2015).

The reduction of Hg pools in many of the organic horizons after the prescribed fire reflects another consequence of fire (Homann et al., 2015; Kolka et al., 2017). The difference between the average Hg pool before and after burning is commonly used to estimate the flux of Hg released into the atmosphere (Harden et al., 2004; Engle et al., 2006; Biswas et al., 2007; Melendez-Perez et al., 2014). Following this approach, the flux of Hg released from soils to air during the prescribed fire was 0.3 g Hg ha^{-1}, which was three and ten times lower than that reported for litter burning by wildfires in forested areas from the western US (Obrist et al., 2009) and the Amazonian rainforest (Melendez-Perez et al., 2014), respectively. These notable differences may be attributed to species-specific features of shrublands and tree-covered forests that determine pre-fire Hg pools (Biswas et al., 2007; Obrist et al., 2016) and the burning temperatures reached during the fire. In addition to their lower efficiency in removing atmospheric Hg compared to tree species, shrubs also transfer less Hg to the soil surface through litterfall due to their smaller aboveground biomass. Consequently, shrubland soils have a lower Hg pool available to be released after a wildfire, which justifies the low estimates of Hg loss obtained in the present study.

The total flux of Hg lost due to prescribed fire was 0.61 g ha^{-1}, resulting from the sum of the Hg released from the burning of organic

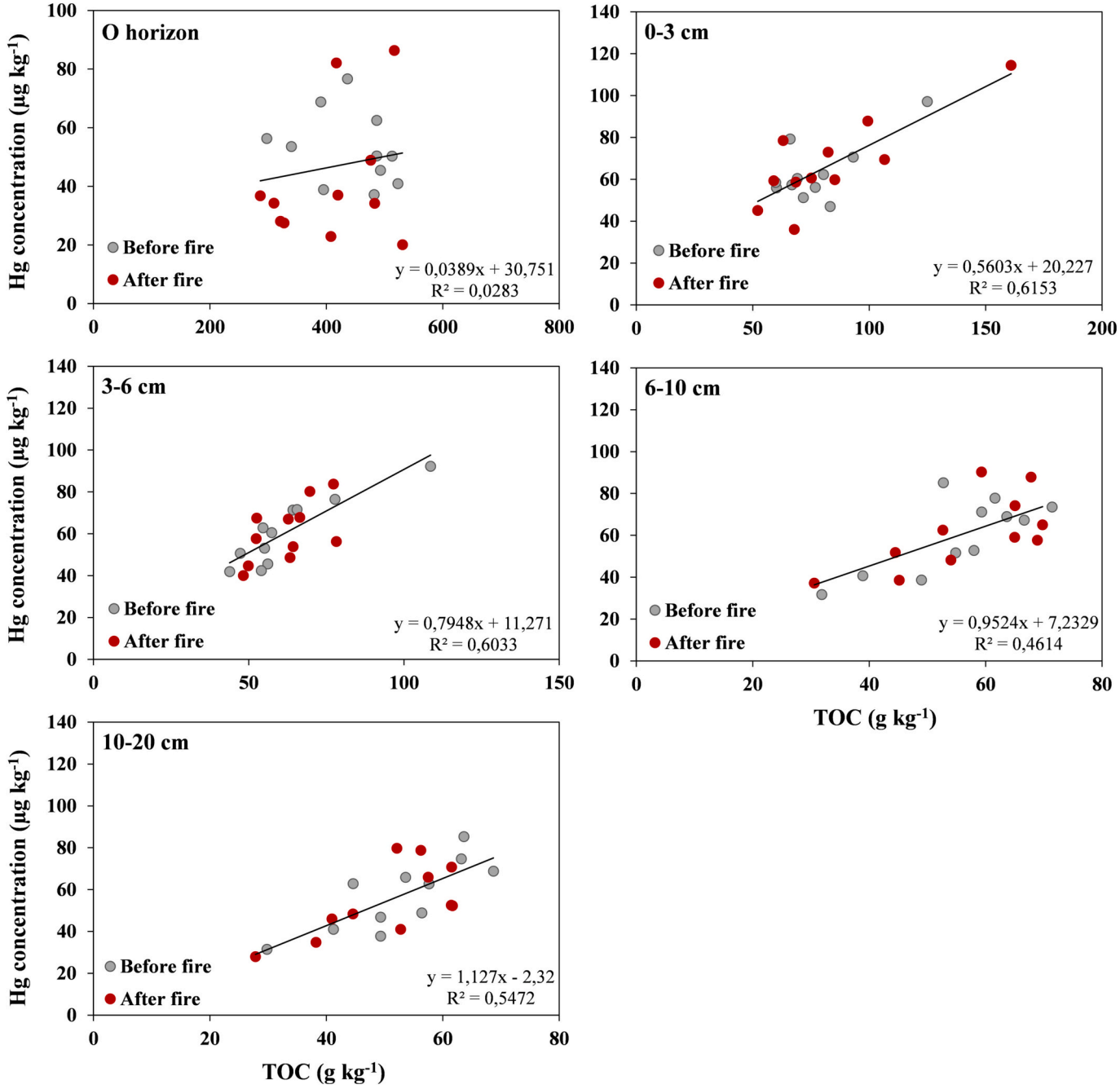

Fig. 6. Regression between Hg and total organic carbon (TOC) concentrations for the different soil layers (O-horizon and several depth intervals of the mineral soil) before and after fire.

horizons and shrubs, as there were no significant losses in the Hg pool of mineral soil layers. This value was of the same order of magnitude as that (0.36 g ha^{-1}) obtained after a wildfire that affected vegetation and litter in a sagebrush area (Engle et al., 2006).

4.2. Fire-induced changes in SOM: biogenic elements (C, N)

The total organic C (TOC) content in unburned O-horizons was quite similar to the average (450 g kg^{-1}) found in organic layers of shrubland soils from NW Spain (Fontúrbel et al., 2016). In the mineral soil, the concentration and vertical pattern of TOC were comparable to those found in mineral soils from shrublands in the northern Iberian Peninsula (Fontúrbel et al., 2016; Rial et al., 2016; Calvo de Anta et al., 2020; Fonseca et al., 2022). The averages of total N and C/N ratio in undisturbed organic horizons were similar to those found by Fontúrbel et al. (2016). Higher C pools in mineral soil layers than in organic horizons are justified by a greater bulk density in the former (0.7–1.0 g cm^{-3}) compared to that of the organic horizons (0.04–0.05 g cm^{-3}) (Table S1), as well as to the low mean thickness in O-horizons (average 1.4 cm).

The diminution of organic C due to fire, confined to occur in the organic horizons and in the 0–3 mineral soil layer, was expected considering a lower effect of temperature with increasing soil depth (Fernández et al., 2008; Mataix-Solera et al., 2011). Moreover, part of the SOM in the uppermost layers of shrubland soils constitutes the unprotected free particulate organic matter fraction, whose low density may accelerate its combustion (Merino et al., 2021). The combination of a lower influence of fire temperature and a more physically protected

OM may explain the absence of a significant reduction of TOC in deeper soil layers. In addition, the heterogeneous distribution of fuel load, the spatial variation of fire temperature and its residence time may also explain why the loss of TOC did not occur throughout all the study area (Santana et al., 2011; Table S2).

The response of TOC to fire in the uppermost mineral soil layers is highly variable, with some studies showing no effects (Fontúrbel et al., 2016; Girona-García et al., 2019), and others evidencing reductions or gains (Úbeda et al., 2005; Girona-García et al., 2018a, 2018c; Fonseca et al., 2022). Soil sampling procedure and the dominant plant species were pointed out to justify variations of TOC in the uppermost mineral soil layers of shrublands (Badía et al., 2017).

The mean loss of TOC after the prescribed fire in the organic horizons and the 0–3 cm mineral soil layer (1–5 %) was low compared to the 38 % reported for similar layers in shrubland soils (Girona-García et al., 2018b, 2019; Merino et al., 2019, 2021). The time in which the prescribed fire took place, its intensity, severity and duration, soil moisture, plant species and cover and the physical protection of SOM were suggested as factors influencing the variation of TOC losses (Girona-García et al., 2018a; Merino et al., 2021).

The slight increase in total N after a fire in many of the studied locations agrees with similar findings on the effects of prescribed fires on shrubland soils (Gómez-Rey et al., 2013; Alcañiz et al., 2016; Fontúrbel et al., 2016; Girona-García et al., 2018a, 2018c, 2019). According to Úbeda et al. (2005), N-rich ash derived from low combustion temperatures in the forest floor may account for total N gains.

The slight decrease in the C/N ratio after the fire, both in organic horizons and mineral soils, coincides with the findings observed in shrubland soils from the Iberian Peninsula (Fontúrbel et al., 2016; Merino et al., 2021). Several factors may explain changes in the C/N ratio, such as the quickest loss of C upon N after the fire (Merino et al., 2021), the immobilization of N in recalcitrant forms favored by fire (González-Pérez et al., 2004) or fire-induced changes in soil microbial parameters (Fontúrbel et al., 2012; Barreiro et al., 2015).

The considerable diminution of the C pool observed in organic horizons after the fire (46 %) was similar to that reported by Vega et al. (2005) in NW Spain during a light burn affecting the forest floor of shrubland. Greater losses of organic C pool (>65 %) were previously reported in the same area (Fonseca et al., 2022) as well as after a prescribed burn in Mediterranean shrubland (Merino et al., 2019). The minor changes in the C pool in the uppermost mineral soil layers can be explained by the isolation effect that organic horizons exert on the mineral soil against fire effects (Kolka et al., 2017; Merino et al., 2019). The increase of C pools at the deepest mineral soil layer (10–20 cm) after fire may be explained by the increase in C concentrations at several of the 11 locations, so the incorporation of charred particles from overlying organic horizons cannot be ruled out (Dai et al., 2006; Merino et al., 2019, 2021; Fonseca et al., 2022).

4.3. Fire-induced changes in Hg and SOM in different size fractions

Mercury distribution in soil aggregates of different sizes before and after the prescribed fire provides some insights about the potential co-mobilization of Hg and soil particles due to erosion. Soil erosion is one of the most concerning consequences of the alteration of soil physical properties due to prescribed fires (Alcañiz et al., 2018). Therefore, soil erosion can be considered a vector for Hg mobilization in burned catchments (Nelson et al., 2007; Burke et al., 2010).

The increasing trend of Hg concentrations with decreasing aggregate size in the unburnt soil samples (O-horizon and 0–3 cm layer) is consistent with findings reported in previous studies (Grigal, 2003; Béliveau et al., 2009; Burke et al., 2010; Qin et al., 2014; Gómez-Armesto et al., 2020). This trend in Hg levels is attributed to the larger specific surface area of the smaller aggregates that favors Hg retention (Fernández-Martínez et al., 2005; Garcia Bravo et al., 2011). Moreover, differences in the chemical composition of SOM among different size fractions may also explain variable Hg levels among them.

The smaller fraction (<0.2 mm) of the organic horizons before fire showed the highest Hg concentration (94 μg kg^{-1}) and the lowest C content (343 g kg^{-1}) together with reduced C/N ratios (27). This suggests that Hg would be more readily retained in aggregates with well-decomposed SOM than in those with higher TOC contents, which is supported by the negative correlations observed for Hg with total C concentration ($r_s = -0.943$; $p < 0.01$; $n = 6$) and the C/N ratio ($r_s = -0.829$; $p < 0.05$; $n = 6$) in different fractions of unburnt organic horizons (Fig. S8). An inversely proportional correlation between Hg and parameters related to SOM (i.e. TOC and C/N) is commonly reported in forest soils (Obrist et al., 2012; Blackwell and Driscoll, 2015; Navrátil et al., 2016; Méndez-López et al., 2022).

In the unburnt 0–3 cm mineral soil layer, Hg levels also increased as aggregate size decreased (from 36 to 85 μg kg^{-1}, Table 2), but no correlations between Hg and TOC or C/N ratio were found. This suggests that Hg could be influenced by inorganic soil compounds such as clay minerals and metal (Fe, Al) oxy-hydroxides that were reported to favor the accumulation of Hg in the mineral soil (Fiorentino et al., 2011; Guedron et al., 2009; Navrátil et al., 2016), influencing the distribution of total Hg among soil aggregates of different size (Do Valle et al., 2005; Xu et al., 2014; Gómez-Armesto et al., 2018).

After the prescribed fire, total Hg and TOC concentrations diminished in all size fractions from the organic horizons (Table 2), as previously reported in shrubland soils affected by moderate-severity wildfires (Girona-García et al., 2018c; Merino et al., 2021). Contrary to unburned samples, Hg concentration did not increase with decreasing aggregate size in O-horizons after the prescribed fire. On the other hand, few changes were observed in total N levels after the fire in the O-horizons and the 0–3 cm soil layer, which can be attributed to a redistribution of N forms among smaller and larger aggregate size fractions (Martí-Roura et al., 2014).

It is noteworthy that, in the organic horizon, the greatest diminution of total Hg (49 %) after the prescribed fire occurred in the smallest fraction assessed (<0.2 mm), which also suffered the greatest TOC diminution (61 %). This contrasts with previous findings reporting preferential combustion of coarse aggregates due to a higher presence of oxygen in their macropores (Jordán et al., 2011). In any case, regardless of aggregate size, the loss of Hg in the burned organic horizons was a direct consequence of organic matter combustion during the fire. This is supported by the fact that the mobilization of Hg bound to organic matter starts at 250 °C (Biester et al., 2002), a temperature widely exceeded in the O-horizon during the prescribed fire (Fig. S2). Moreover, the considerable diminution of Hg in the smallest fraction of O-horizons during fire could be explained by their higher sensitivity to fire compared to coarser aggregates. In this regard, Girona-García et al. (2018c) indicated that organic C levels in finer fractions (<0.25 mm) were strongly influenced by fire compared to coarser fractions. In addition, TOC loss was also related to the breakdown of soil aggregates (Merino et al., 2021) and to the effect of soil water repellency (Jiménez-Morillo et al., 2016, 2017, 2022) that increases soil erodibility (Mataix-Solera et al., 2011). These facts reinforce the threat of Hg mobilization after the fire. Due to the great erosion potential of burned sites, Hg could be mobilized to surface waters bound to organic or particulate matter (Burke et al., 2010). In fact, Jensen et al. (2017) found great concentrations of particulate Hg in water samples from burned areas after high-flow events and Burton et al. (2016) attributed the higher Hg levels in stormflow water samples to leaching of soil particles during runoff from burned areas.

Contrary to the organic horizons, all size fractions from the 0–3 cm mineral soil layer showed higher Hg concentrations after the fire, being consistent with the increase of total C concentrations. Thus, debris of total or partially burned material of the organic horizons can explain the increase in total C (Jiménez-Morillo et al., 2016; Badía et al., 2017). These debris would increase Hg concentrations in the uppermost mineral soil layers after fire, as in locations 3, 6 and 10 (Fig. S3), by

replenishing the mass of Hg not volatilized during the fire. Such increase in Hg concentration in mineral topsoil aggregates following fire also occurred in burned areas where bare soil is susceptible to erosion transferring Hg to freshwater ecosystems where its potential toxicity increases (Woodruff and Cannon, 2010). The lack of significant variations between before and after the fire in the C/N ratio of the fractions assessed in the 0–3 cm mineral soil layer suggests a secondary role of organic matter quality influencing Hg increases at such depth. Similarly, minor changes in the C/N ratios due to burning in different size fractions of shrubland soil affected by fire were also observed by Martí-Roura et al. (2014).

4.4. Hg related to SOM molecular composition in different soil layers and size fractions

In summary, the results obtained suggest that the variable quality of SOM among different aggregate size fractions in different soil layers leads to variable capacity for Hg retention. This fact together with the changes induced by fire in SOM and Hg contents showed the need for further research on organic matter composition and how this parameter may affect the presence and retention of Hg depending on soil aggregate size.

The preliminary molecular study done by FT-IR spectroscopy showed specific differences among soil layers, particle size fractions and times relative to the prescribed fire (Figs. 3, S5 and S6). The FT-IR spectra of unaffected SOM in a specific soil layer and its different particle size fractions depicted the same infrared profile. These samples showed a band at 2900 cm^{-1} characteristic of the alkylic compounds (Miralles et al., 2007), which is unique in non-affected samples. The presence of these lipid-like compounds may come from i) epicuticular waxes (fresh biomass deposition), ii) microbial degradation of plant biomass, or iii) microbial cells (Jiménez-Morillo et al., 2016, 2017, 2018). The absence of this band in SOM at different soil layers and particle size fractions after the prescribed fire may indicate the thermal destruction of the lipidic fraction of soil, which has been observed by Jiménez-Morillo et al. (2017, 2020). Another important result was the higher intensity of the band corresponding to the amide II group (at 1490 cm^{-1}), only in the finest soil fraction (<0.2 mm) after the fire. This change may indicate an accumulation of protein-derived compounds (peptides) generated by the denaturalization of proteins or the destruction of membrane cells by fire (González-Pérez et al., 2004; Jiménez-Morillo et al., 2018). These molecular differences may be correlated to the significant differences in the VIP FT-IR bands used by the generation of the forecasting Hg concentration models (Fig. 4). A detailed examination of the VIP values for each PLS models showed that the Hg concentration in O-horizon before fire was significantly linked to lipid-like compounds (2900 cm^{-1}), aromatic-derived (1640 cm^{-1}), protein-derived (1490 cm^{-1}), lignin-like compounds (1160 cm^{-1}) and some ester and alcohol molecules (1000 cm^{-1}). In contrast, fire-affected O-horizon were dominated by bands at 1640, 1100, and 910 cm^{-1} (aromatics and lignin-like compounds, respectively). In the case of 0–3 cm depth layer, the dominant VIP bands of unburned SOM were assigned to protein-derived (1490 cm^{-1}), and lignin (1100, 1000 and 910 cm^{-1}) compounds, while for fire-affected SOM the significant biogenic families were lignin-like (1100 and 910 cm^{-1}) compounds. These results may confirm that the quality (molecular composition) of SOM before and after prescribed fires is a significant and remarkable variable to assess and predict the alteration of Hg concentration after wildfires and prescribed burnings. The use of IR spectra from burned and unburned bulk soil samples from different layers allowed the validation of predictive Hg models (Fig. 5). Thus, there were no significant variations in the different scenarios (BF and AF) and layers (O-horizon and 0–3 cm) assessed, with the exception of the burned O-horizon. This validation of the model suggests that it is suitable for use with real samples; nevertheless, as it is a preliminary model, it is required to increase the number of "control" and "training" samples to cover a wider range of scenarios. Therefore, despite being a preliminary work, we can conclude that the application of FT-IR spectroscopy and chemometric analysis is an appropriate approach not only for predicting changes in Hg content but also for evaluating the chemical groups that can form linkages with Hg. The evaluation of the correlation between the main individual chemical families with Hg concentration will be the main focus of the next work, in which we will try to combine ultra-high resolution analytical pyrolysis (Py-GC/Q-TOF) with chemometrics. This work has allowed us to verify our hypothesis that SOM quality may be considered an important factor in the biogeochemical cycle of Hg.

5. Conclusions

Low-severity fires are able to destabilize Hg in soils, leading to its redistribution in the environment, as expected due to the significant changes detected in the organic horizon. The higher Hg levels found in the smallest aggregates in the uppermost soil layers are of particular concern because of their readiness to mobilize during erosion and the potential to reach watercourses, where Hg is more susceptible to convert into methylmercury. Mineral soils are reinforced as long-term Hg reservoirs where Hg is shielded from external disturbances since no significant changes due to burning were observed. However, large uncertainties in regional and global estimates of Hg loading by wildfires are suspected due to the large variability in post-fire Hg losses and gains at a local scale in the uppermost soil layers.

The molecular characterization of SOM in combination with multivariate statistical analysis showed the significant impact of SOM quality on the retention/emission of Hg, as well as the main organic families to which Hg is attached under different scenarios (before and after the prescribed fire). The forecasted Hg values obtained by the models generated in this study will aid as a starting point for future research into the dynamics of Hg biogeochemical cycling in terrestrial ecosystems and how it is affected by natural and anthropogenic disturbances.

CRediT authorship contribution statement

Melissa Méndez-López: Conceptualization, Methodology, Data curation, Visualization, Formal analysis, Investigation, Writing – original draft, Writing – review & editing. **Nicasio Tomás Jiménez-Morillo:** Methodology, Data curation, Formal analysis, Investigation, Writing – original draft, Writing – review & editing. **Felicia Fonseca:** Data curation, Investigation, Visualization, Writing – review & editing. **Tomás de Figueiredo:** Data curation, Investigation, Visualization, Writing – review & editing. **Andrea Parente-Sendín:** Writing – original draft, Visualization, Data curation. **Flora Alonso-Vega:** Writing – original draft, Funding acquisition, Resources, Visualization, Supervision, Writing – review & editing. **Manuel Arias-Estévez:** Funding acquisition, Visualization, Resources, Supervision, Project administration. **Juan Carlos Nóvoa-Muñoz:** Conceptualization, Formal analysis, Visualization, Resources, Writing – original draft, Supervision, Writing – review & editing, Funding acquisition, Project administration.

Declaration of competing interest

The authors declare that they have no known competing financial interests or personal relationships that could have appeared to influence the work reported in this paper.

Data availability

Data will be made available on request.

Acknowledgments

This work was supported by the Interreg V-A Spain-Portugal program (POCTEP) 2014–2020 (Project 0701_TERRAMATER_1_E) funded

by the European Regional Development Fund (FEDER), the EROFIRE project (PCIF/RPG/0079/2018) funded by FCT, Portugal and the InMerForEcos project (PID 2021-125114OB-I00) funded by Ministerio de Ciencia e Innovación and Agencia Estatal de Investigación (MCIN/AEI) and FEDER. M. Méndez-López was supported by the predoctoral grant FPU (FPU17/05484) funded by the Ministerio de Educación y Formación Profesional. N.T. Jiménez-Morillo was supported by a "Ramón y Cajal" contract (RYC2021-031253-I) funded by MCIN/AEI/10.13039/501100011033 and the European Union "NextGenerationEU"/PRTR". The financial support of the Consellería de Cultura, Educación e Universidade (Xunta de Galicia) through the contract ED431C2021/46-GRC granted to the research group BV1 of the University of Vigo is also recognized. Open-access funding for this research has been provided by the University of Vigo/CISUG.

Appendix A. Supplementary data

Supplementary data to this article can be found online at https://doi.org/10.1016/j.scitotenv.2023.167532.

References

Abraham, J., Dowling, K., Florentine, S., 2018. Effects of prescribed fire and post-fire rainfall on mercury mobilization and subsequent contamination assessment in a legacy mine site in Victoria, Australia. Chemosphere 190, 144–153. https://doi.org/10.1016/j.chemosphere.2017.09.117.

Alcañiz, M., Outeiro, L., Francos, M., Farguell, J., Úbeda, X., 2016. Long-term dynamics of soil chemical properties after a prescribed fire in a Mediterranean forest (Montgrí Massif, Catalonia, Spain). Sci. Total Environ. 572, 1329–1335. https://doi.org/10.1016/j.scitotenv.2016.01.115.

Alcañiz, M., Outeiro, L., Francos, M., Úbeda, X., 2018. Effects of prescribed fires on soil properties: a review. Sci. Total Environ. 613–614, 944–957. https://doi.org/10.1016/j.scitotenv.2017.09.144.

Almendros, G., González-Vila, F.J., Martin, F., 1990. Fire-induced transformation of soil organic matter from an oak forest: an experimental approach to the effects of fire on humic substances. Soil Sci. 149, 158–168. https://doi.org/10.1097/00010694-199003000-00005.

Badía, D., López-García, S., Martí, C., Ortíz-Perpiñá, O., Girona-García, A., Casanova-Gascón, J., 2017. Burn effects on soil properties associated to heat transfer under contrasting moisture content. Sci. Total Environ. 601–602, 1119–1128. https://doi.org/10.1016/j.scitotenv.2017.05.254.

Badía-Villas, D., González-Pérez, J.A., Aznar, J.M., Arjona-Gracia, B., Martí-Dalmau, C., 2014. Changes in water repellency, aggregation and organic matter of a mollic horizon burned in laboratory: soil depth affected by fire. Geoderma 213, 400–407. https://doi.org/10.1016/j.geoderma.2013.08.038.

Barreiro, A., Fontúrbel, M.T., Lombao, A., Martín, A., Vega, J.A., Fernández, C., Carballas, T., Díaz-Raviña, M., 2015. Using phospholipid fatty acid and community level physiological profiling techniques to characterize soil microbial communities following an experimental fire and different stabilization treatments. Catena 135, 419–429. https://doi.org/10.1016/j.catena.2014.07.011.

Béliveau, A., Lucotte, M., Davidson, R., do Canto Lopes, L.O., Paquet, S., 2009. Early Hg mobility in cultivated tropical soils one year after slash-and-burn of the primary forest, in the Brazilian Amazon. Sci. Total Environ. 407, 4480–4489. https://doi.org/10.1016/j.scitotenv.2009.04.012.

Biester, H., Scholz, C., 1997. Determination of mercury binding forms in contaminated soils: mercury pyrolysis versus sequential extractions. Environ. Sci. Technol. 31, 233–239. https://doi.org/10.1021/es960369h.

Biester, H., Müller, G., Schöler, H.F., 2002. Binding and mobility of mercury in soils contaminated by emissions from chlor-alkali plants. Sci. Total Environ. 284, 191–203. https://doi.org/10.1016/S0048-9697(01)00885-3.

Biswas, A., Blum, J.D., Klaue, B., Keeler, G.J., 2007. Release of mercury from rocky mountain forest fires. Global Biogeochem. Cycles 21. https://doi.org/10.1029/2006GB002696.

Biswas, A., Blum, J.D., Keeler, G.J., 2008. Mercury storage in surface soils in a central Washington forest and estimated release during the 2001 Rex Creek Fire. Sci. Total Environ. 404, 129–138. https://doi.org/10.1016/j.scitotenv.2008.05.043.

Blackwell, B.D., Driscoll, C.T., 2015. Deposition of mercury in forests along a montane elevation gradient. Environ. Sci. Technol. 49, 5363–5370. https://doi.org/10.1021/es505928w.

Burke, M.P., Hogue, T.S., Ferreira, M., Mendez, C.B., Navarro, B., Lopez, S., Jay, J.A., 2010. The effect of wildfire on soil mercury concentrations in Southern California Watersheds. Water Air Soil Pollut. 212, 369–385. https://doi.org/10.1007/s11270-010-0351-y.

Burton, C.A., Hoefen, T.M., Plumlee, G.S., Baumberger, K.L., Backlin, A.R., Gallegos, E., Fisher, R.N., 2016. Trace elements in stormflow, ash, and burned soil following the 2009 station fire in Southern California. PLoS One 11. https://doi.org/10.1371/journal.pone.0153372.

Calvo de Anta, R., Luís, E., Febrero-Bande, M., Galiñanes, J., Macías, F., Ortíz, R., Casás, F., 2020. Soil organic carbon in peninsular Spain: influence of environmental factors and spatial distribution. Geoderma 370. https://doi.org/10.1016/j.geoderma.2020.114365.

Campos, I., Vale, C., Abrantes, N., Keizer, J.J., Pereira, P., 2015. Effects of wildfire on mercury mobilisation in eucalypt and pine forests. Catena 131, 149–159. https://doi.org/10.1016/j.catena.2015.02.024.

Clarkson, T.W., Magos, L., 2006. The toxicology of mercury and its chemical compounds. Crit. Rev. Toxicol. 36, 609–662. https://doi.org/10.1080/10408440600845619.

Coradeschi, G., Jiménez-Morillo, N.T., Dias, C.B., Beltrame, M., Belo, A.D.F., Granged, A. J.P., Sadori, L., Valera, A., 2023. Anthracological study of a Chalcolithic funerary deposit from Perdigões (Alentejo, Portugal): a new analytical methodology to establish the wood burning temperature. PLoS One 18 (7), e0287531. https://doi.org/10.1371/journal.pone.0287531.

Dai, X., Boutton, T.W., Hailemichael, M., Ansley, R.J., Jessup, K.E., 2006. Soil carbon and nitrogen storage in response to fire in a temperate mixed-grass savanna. J. Environ. Qual. 35, 1620–1628. https://doi.org/10.2134/jeq2005.0260.

De la Rosa, J.M., Jiménez-González, M.A., Jiménez-Morillo, N.T., Knicker, H., Almendros, G., 2019. Quantitative forecasting black (pyrogenic) carbon in soils by chemometric analysis of infrared spectra. J. Environ. Manag. 251 https://doi.org/10.1016/j.jenvman.2019.109567.

Do Valle, C.M., Santana, G.P., Augusti, R., Egreja Filho, F.B., Windmöller, C.C., 2005. Speciation and quantification of mercury in Oxisol, Ultisol, and Spodosol from Amazon (Manaus, Brazil). Chemosphere 58, 779–792. https://doi.org/10.1016/j.chemosphere.2004.09.005.

Dorez, G., Ferry, L., Sonnier, R., Taguet, A., Lopez-Cuesta, J.-M., 2014. Effect of cellulose, hemicellulose and lignin contents on pyrolysis and combustion of natural fibers. J. Anal. Appl. Pyrolysis 107, 323–331. https://doi.org/10.1016/j.jaap.2014.03.017.

Dupuis, T., Jambu, P., 1969. Etude par spectrographie infrarouge des produits de l'humification 627 en milieu hydromorphe calcique. Science du Sol 1, 23–35.

Engle, M.A., Gustin, M.S., Johnson, D.W., Murphy, J.F., Miller, W.W., Walker, R.F., Wright, J., Markee, M., 2006. Mercury distribution in two Sierran forest and one desert sagebrush steppe ecosystems and the effects of fire. Sci. Total Environ. 367, 222–233.

Fernández, C., Vega, J.A., Fonturbel, T., Jiménez, E., Pérez, J.R., 2008. Immediate effects of prescribed burning, chopping and clearing on runoff, infiltration and erosion in a shrubland area in Galicia (NW Spain). L. Degrad. Dev. 19, 502–515. https://doi.org/10.1002/ldr.855.

Fernández-Martínez, R., Loredo, J., Ordóñez, A., Rucandio, M.I., 2005. Distribution and mobility of mercury in soils from an old mining area in Mieres, Asturias (Spain). Sci. Total Environ. 346, 200–212. https://doi.org/10.1016/j.scitotenv.2004.12.010.

Fiorentino, J.C., Enzweiler, J., Angélica, R.S., 2011. Geochemistry of mercury along a soil profile compared to other elements and to the parental rock: evidence of external input. Water Air Soil Pollut. 221, 63–75. https://doi.org/10.1007/s11270-011-0769-x.

Fonseca, F., Silva, D., Bueno, P., Hernández, Z., Royer, A.C., de Figueiredo, T., 2022. Temporal dynamics of carbon storage in a Mediterranean mountain scrubland managed by prescribed fire. Catena 212. https://doi.org/10.1016/j.catena.2022.106107.

Fontúrbel, M.T., Barreiro, A., Vega, J.A., Martín, A., Jiménez, E., Carballas, T., Fernández, C., Díaz-Raviña, M., 2012. Effects of an experimental fire and post-fire stabilization treatments on soil microbial communities. Geoderma 191, 51–60. https://doi.org/10.1016/j.geoderma.2012.01.037.

Fontúrbel, M.T., Fernández, C., Vega, J.A., 2016. Prescribed burning versus mechanical treatments as shrubland management options in NW Spain: mid-term soil microbial response. Appl. Soil Ecol. 107, 334–346. https://doi.org/10.1016/j.apsoil.2016.07.008.

Garcia Bravo, A., Bouchet, S., Amouroux, D., Poté, J., Dominik, J., 2011. Distribution of mercury and organic matter in particle-size classes in sediments contaminated by a waste water treatment plant: Vidy Bay, Lake Geneva, Switzerland. J. Environ. Monit. 13, 974–982. https://doi.org/10.1039/c0em00534g.

Girona-García, A., Badía-Villas, D., Martí-Dalmau, C., Ortiz-Perpiñá, O., Mora, J.L., Armas-Herrera, C.M., 2018a. Effects of prescribed fire for pasture management on soil organic matter and biological properties: a 1-year study case in the Central Pyrenees. Sci. Total Environ. 618, 1079–1087. https://doi.org/10.1016/j.scitotenv.2017.09.127.

Girona-García, A., Ortiz-Perpiñá, O., Badía-Villas, D., Martí-Dalmau, C., 2018b. Effects of prescribed burning on soil organic C, aggregate stability and water repellency in a subalpine shrubland: variations among sieve fractions and depths. Catena 166, 68–77. https://doi.org/10.1016/j.catena.2018.03.018.

Girona-García, A., Zufiaurre Galarza, R., Mora, J.L., Armas-Herrera, C.M., Martí, C., Ortiz-Perpiñá, O., Badía-Villas, D., 2018c. Effects of prescribed burning for pasture reclamation on soil chemical properties in subalpine shrublands of the Central Pyrenees (NE-Spain). Sci. Total Environ. 644, 583–593. https://doi.org/10.1016/j.scitotenv.2018.06.363.

Girona-García, A., Ortiz-Perpiñá, O., Badía-Villas, D., 2019. Dynamics of topsoil carbon stocks after prescribed burning for pasture restoration in shrublands of the Central Pyrenees (NE-Spain). J. Environ. Manag. 233, 695–705. https://doi.org/10.1016/j.jenvman.2018.12.057.

Gómez-Armesto, A., Méndez-López, M., Pontevedra-Pombal, X., García-Rodeja, E., Moretto, A., Estévez-Arias, M., Nóvoa-Muñoz, J.C., 2020. Mercury accumulation in soil fractions of podzols from two contrasted geographical temperate areas: southwest Europe and southernmost America. Geoderma 362. https://doi.org/10.1016/j.geoderma.2019.114120.

Gómez-Armesto, A.G., Bibián-Núñez, L., Campillo-Cora, C., Pontevedra-Pombal, X., Arias-Estévez, M., Nóvoa-Muñoz, J.C., 2018. Total mercury distribution among soil aggregate size fractions in a temperate forest podzol | Distribuição do mercúrio total em função da dimensão dos agregados num podzol de floresta temperada |

Distribución de mercurio total en función del tamaño de agr. Spanish J. Soil Sci. 8, 57–73. https://doi.org/10.3232/SJSS.2018.V8.N1.05.
Gómez-Rey, M.X., Couto-Vázquez, A., García-Marco, S., González-Prieto, S.J., 2013. Impact of fire and post-fire management techniques on soil chemical properties. Geoderma 195–196, 155–164. https://doi.org/10.1016/j.geoderma.2012.12.005.
González-Pérez, J.A., González-Vila, F.J., Almendros, G., Knicker, H., 2004. The effect of fire on soil organic matter - a review. Environ. Int. 30, 855–870. https://doi.org/10.1016/j.envint.2004.02.003.
Grigal, D.F., 2003. Mercury sequestration in forests and peatlands: a review. J. Environ. Qual. 32, 393–405.
Gruba, P., Socha, J., Pietrzykowski, M., Pasychnyk, D., 2019. Tree species affects the concentration of total mercury (Hg) in forest soils: evidence from a forest soil inventory in Poland. Sci. Total Environ. 647, 141–148. https://doi.org/10.1016/j.scitotenv.2018.07.452.
Guedron, S., Grangeon, S., Lanson, B., Grimaldi, M., 2009. Mercury speciation in a tropical soil association; consequence of gold mining on Hg distribution in French Guiana. Geoderma 153, 331–346. https://doi.org/10.1016/j.geoderma.2009.08.017.
Harden, J.W., Neff, J.C., Sandberg, D.V., Turetsky, M.R., Ottmar, R., Gleixner, G., Fries, T.L., Manies, K.L., 2004. Chemistry of burning the forest floor during the FROSTFIRE experimental burn, interior Alaska, 1999. Global Biogeochem. Cycles 18. https://doi.org/10.1029/2003GB002194.
Hasan, M.I., Masoud, M.S., 2014. Thermal analysis (TGA), diffraction thermal analysis (DTA), infrared and X-rays analysis for sediment samples of Toubrouk city (Libya) coast. Int. J. Chem. Sci. 12, 11–22.
Homann, P.S., Darbyshire, R.L., Bormann, B.T., Morrissette, B.A., 2015. Forest structure affects soil mercury losses in the presence and absence of wildfire. Environ. Sci. Technol. 49, 12714–12722. https://doi.org/10.1021/acs.est.5b03355.
IPCC (Intergovernmental Panel on Climate Change), 2013. Climate change 2013: the physical science basis. In: Stocker, T.F., Qin, D., Plattner, G.-H., Tignor, M.M.B., Allen, S.K., Boschung, J., Nauels, A., Xia, Y., Bex, V., Midgley, P.M. (Eds.), Contributions of Working Group I to the Fifth Assessment Report of the Intergovernmental Panel on Climate Change. Cambridge University Press, Cambridge, United Kingdom and New York, NY, USA.
IUSS Working Group WRB, 2022. World Reference Base for Soil Resources. International Soil Classification System for Naming Soils and Creating Legends for Soil Maps (4th ed.). International Union of Soil Sciences (IUSS), Vienna, Austria, 234 pp.
Jensen, A.M., Scanlon, T.M., Riscassi, A.L., 2017. Emerging investigator series: the effect of wildfire on streamwater mercury and organic carbon in a forested watershed in the southeastern United States. Environ Sci Process Impacts 19, 1505–1517. https://doi.org/10.1039/c7em00419b.
Jiménez-González, M.A., Álvarez, A.M., Carral, P., Almendros, G., 2019. Chemometric assessment of soil organic matter storage and quality from humic acid infrared spectra. Sci. Total Environ. 685, 1160–1168. https://doi.org/10.1016/j.scitotenv.2019.06.231.
Jiménez-Morillo, N.T., de la Rosa, J.M., Waggoner, D., Almendros, G., González-Vila, F. J., González-Pérez, J.A., 2016. Fire effects in the molecular structure of soil organic matter fractions under Quercus suber cover. Catena 145, 266–273. https://doi.org/10.1016/j.catena.2016.06.022.
Jiménez-Morillo, N.T., Spangenberg, J.E., Miller, A.Z., Jordán, A., Zavala, L.M., González-Vila, F.J., González-Pérez, J.A., 2017. Wildfire effects on lipid composition and hydrophobicity of bulk soil and soil size fractions under Quercus suber cover (SW-Spain). Environ. Res. 159, 394–405. https://doi.org/10.1016/j.envres.2017.08.022.
Jiménez-Morillo, N.T., González-Pérez, J.A., Almendros, G., De la Rosa, J.M., Waggoner, D.C., Jordán, A., Zavala, L.M., González-Vila, F.J., Hatcher, P.G., 2018. Ultra-high resolution mass spectrometry of physical speciation patterns of organic matter in fire-affected soils. J. Environ. Manag. 225, 139–147. https://doi.org/10.1016/j.jenvman.2018.07.069.
Jiménez-Morillo, N.T., Almendros, G., De la Rosa, J.M., Jordán, A., Zavala, L.M., Granged, A.J.P., González-Pérez, J.A., 2020. Effect of a wildfire and of post-fire restoration actions in the organic matter structure in soil fractions. Sci. Total Environ. 728 https://doi.org/10.1016/j.scitotenv.2020.138715.
Jiménez-Morillo, N.T., Almendros, G., Miller, A.Z., Hatcher, P.G., González-Pérez, J.A., 2022. Hydrophobicity of soils affected by fires: an assessment using molecular markers from ultra-high resolution mass spectrometry. Sci. Total Environ. 817. https://doi.org/10.1016/j.scitotenv.2022.152957.
Johnson, D.W., Curtis, P.S., 2001. Effects of forest management on soil C and N storage: meta analysis. For. Ecol. Manag. 140, 227–238. https://doi.org/10.1016/S0378-1127(00)00282-6.
Jordán, A., Zavala, L.M., Mataix-Solera, J., Nava, A.L., Alanís, N., 2011. Effect of fire severity on water repellency and aggregate stability on Mexican volcanic soils. Catena 84, 136–147. https://doi.org/10.1016/j.catena.2010.10.007.
Knicker, H., González-Vila, F.J., Polvillo, O., González, J.A., Almendros, G., 2005. Fire-induced transformation of C- and N- forms in different organic soil fractions from a Dystric Cambisol under a Mediterranean pine forest (Pinus pinaster). Soil Biol. Biochem. 37, 701–718. https://doi.org/10.1016/j.soilbio.2004.09.008.
Kolka, R., Sturtevant, B., Townsend, P., Miesel, J., Wolter, P., Fraver, S., DeSutter, T., 2014. Post-fire comparisons of forest floor and soil carbon, nitrogen, and mercury pools with fire severity indices. Soil Sci. Soc. Am. J. 78, S58–S65. https://doi.org/10.2136/sssaj2013.08.0351nafsc.
Kolka, R.K., Sturtevant, B.R., Miesel, J.R., Singh, A., Wolter, P.T., Fraver, S., Desutter, T. M., Townsend, P.A., 2017. Emissions of forest floor and mineral soil carbon, nitrogen and mercury pools and relationships with fire severity for the Pagami Creek Fire in the Boreal Forest of northern Minnesota. Int. J. Wildland Fire 26, 296–305. https://doi.org/10.1071/WF16128.
Kumar, A., Wu, S., Huang, Y., Liao, H., Kaplan, J.O., 2018. Mercury from wildfires: global emission inventories and sensitivity to 2000–2050 global change. Atmos. Environ. 173, 6–15. https://doi.org/10.1016/j.atmosenv.2017.10.061.
Li, X., Wang, X., Yuan, W., Lu, Z., Wang, D., 2022. Increase of litterfall mercury input and sequestration during decomposition with a montane elevation in Southwest China. Environ. Pollut. 292, 118449.
Martí-Roura, M., Rovira, P., Casals, P., Romanyà, J., 2014. Post-fire mineral N allocation and stabilisation in soil particle size fractions in Mediterranean grassland and shrubland. Soil Biol. Biochem. 75, 124–132. https://doi.org/10.1016/j.soilbio.2014.04.009.
Mataix-Solera, J., Cerdà, A., Arcenegui, V., Jordán, A., Zavala, L.M., 2011. Fire effects on soil aggregation: a review. Earth-Sci. Rev. 109, 44–60. https://doi.org/10.1016/j.earscirev.2011.08.002.
Mazur, M., Mitchell, C.P.J., Eckley, C.S., Eggert, S.L., Kolka, R.K., Sebestyen, S.D., Swain, E.B., 2014. Gaseous mercury fluxes from forest soils in response to forest harvesting intensity: a field manipulation experiment. Sci. Total Environ. 496, 678–687. https://doi.org/10.1016/j.scitotenv.2014.06.058.
McCarthy, P., Rice, J.A., 1985. Spectroscopic methods (other than NMR) for determining functionality in humic substances. In: Aiken, G.R., et al. (Eds.), Humic Substances in Soil, Sediment, and Water. Wiley, New York, pp. 527–559.
Meili, M., 1991. The coupling of mercury and organic matter in the biogeochemical cycle - towards a mechanistic model for the boreal forest zone. Water Air Soil Pollut. 56, 333–347. https://doi.org/10.1007/BF00342281.
Melendez-Perez, J.J., Fostier, A.H., Carvalho, J.A., Windmöller, C.C., Santos, J.C., Carpi, A., 2014. Soil and biomass mercury emissions during a prescribed fire in the Amazonian rain forest. Atmos. Environ. 96, 415–422. https://doi.org/10.1016/j.atmosenv.2014.06.032.
Méndez-López, M., Gómez-Armesto, A., Alonso-Vega, F., Pontevedra-Pombal, X., Fonseca, F., de Figueiredo, T., Arias-Estévez, M., Nóvoa-Muñoz, J.C., 2022. The role of afforestation species as a driver of Hg accumulation in organic horizons of forest soils from a Mediterranean mountain area in SW Europe. Sci. Total Environ. 827 https://doi.org/10.1016/j.scitotenv.2022.154345.
Merino, A., Jiménez, E., Fernández, C., Fontúrbel, M.T., Campo, J., Vega, J.A., 2019. Soil organic matter and phosphorus dynamics after low intensity prescribed burning in forests and shrubland. J. Environ. Manag. 234, 214–225. https://doi.org/10.1016/j.jenvman.2018.12.055.
Merino, A., García-Oliva, F., Fontúrbel, M.T., Vega, J.A., 2021. The high content of mineral-free organic matter in soils increases their vulnerability to wildfire in humid-temperate zones. Geoderma 395. https://doi.org/10.1016/j.geoderma.2021.115043.
Miralles, I., Ortega, R., Sánchez-Marañón, M., Soriano, M., Almendros, G., 2007. Assessment of biogeochemical trends in soil organic matter sequestration in Mediterranean calcimorphic mountain soils (Almería, Southern Spain). Soil Biol. Biochem. 39, 2459–2470.
Moreira, F., Viedma, O., Arianoutsou, M., Curt, T., Koutsias, N., Rigolot, E., Barbati, A., Corona, P., Vaz, P., Xanthopoulos, G., Mouillot, F., Bilgili, E., 2011. Landscape - wildfire interactions in southern Europe: implications for landscape management. J. Environ. Manag. 92, 2389–2402. https://doi.org/10.1016/j.jenvman.2011.06.028.
Navrátil, T., Shanley, J., Rohovec, J., Hojdová, M., Penížek, V., Buchtová, J., 2014. Distribution and pools of mercury in Czech forest soils. Water Air Soil Pollut. 225 https://doi.org/10.1007/s11270-013-1829-1.
Navrátil, T., Shanley, J.B., Rohovec, J., Oulehle, F., Šimecek, M., Houška, J., Cudlín, P., 2016. Soil mercury distribution in adjacent coniferous and deciduous stands highly impacted by acid rain in the Ore Mountains, Czech Republic. Appl. Geochem. 75, 63–75. https://doi.org/10.1016/j.apgeochem.2016.10.005.
Nelson, S.J., Johnson, K.B., Kahl, J.S., Haines, T.A., Fernandez, I.J., 2007. Mass balances of mercury and nitrogen in burned and unburned forested watersheds at Acadia National Park, Maine, USA. Environ. Monit. Assess. 126, 69–80. https://doi.org/10.1007/s10661-006-9332-4.
Obrist, D., Johnson, D.W., Lindberg, S.E., 2009. Mercury concentrations and pools in four sierra nevada forest sites, and relationships to organic carbon and nitrogen. Biogeosciences. https://doi.org/10.5194/bg-6-765-2009.
Obrist, D., Johnson, D.W., Edmonds, R.L., 2012. Effects of vegetation type on mercury concentrations and pools in two adjacent coniferous and deciduous forests. J. Plant Nutr. Soil Sci. 175, 68–77. https://doi.org/10.1002/jpln.201000415.
Obrist, D., Pokharel, A.K., Moore, C., 2014. Vertical profile measurements of soil air suggest immobilization of gaseous elemental mercury in mineral soil. Environ. Sci. Technol. 48, 2242–2252. https://doi.org/10.1021/es4048297.
Obrist, D., Pearson, C., Webster, J., Kane, T., Lin, C.-J., Aiken, G.R., Alpers, C.N., 2016. A synthesis of terrestrial mercury in the western United States: spatial distribution defined by land cover and plant productivity. Sci. Total Environ. 568, 522–535. https://doi.org/10.1016/j.scitotenv.2015.11.104.
Ojima, J., 2003. Determining of crystalline silica in respirable dust samples by infrared spectrophotometry in the presence of interferences. J. Occup. Health 45, 94–103.
Olson, C.I., Geyman, B.M., Thackray, C.P., Krabbenhoft, D.P., Tate, M.T., Sunderland, E. M., Driscoll, C.T., 2022. Mercury in soils of the conterminous United States: patterns and pools. Environ. Res. Lett. 17 https://doi.org/10.1088/1748-9326/ac79c2.
Parsons, A., Robichaud, P.R., Lewis, S.A., Napper, C., Clark, J.T., 2010. Field guide for mapping post-fire soil burn severity. USDA For. Serv. - Gen. Tech. Rep. RMRS-GTR 1–49.
Qin, F., Ji, H., Li, Q., Guo, X., Tang, L., Feng, J., 2014. Evaluation of trace elements and identification of pollution sources in particle size fractions of soil from iron ore areas along the Chao River. J. Geochem. Explor. 138, 33–49. https://doi.org/10.1016/j.gexplo.2013.12.005.

Ravichandran, M., 2004. Interactions between mercury and dissolved organic matter - a review. Chemosphere 55, 319–331. https://doi.org/10.1016/j.chemosphere.2003.11.011.

Rial, M., Cortizas, A.M., Rodríguez-Lado, L., 2016. Mapping soil organic carbon content using spectroscopic and environmental data: a case study in acidic soils from NW Spain. Sci. Total Environ. 539, 26–35. https://doi.org/10.1016/j.scitotenv.2015.08.088.

Santana, V.M., Baeza, M.J., Vallejo, V.R., 2011. Fuel structural traits modulating soil temperatures in different species patches of Mediterranean Basin shrublands. Int. J. Wildland Fire 20, 668–677. https://doi.org/10.1071/WF10083.

Sigler, J.M., Lee, X., Munger, W., 2003. Emission and long-range transport of gaseous mercury from a large-scale Canadian boreal forest fire. Environ. Sci. Technol. 37, 4343–4347. https://doi.org/10.1021/es026401r.

Skyllberg, U., 2010. Mercury biogeochemistry in soils and sediments. Dev. Soil Sci. 34, 379–410.

Skyllberg, U., Qian, J., Frech, W., Xia, K., Bleam, W.F., 2003. Distribution of mercury, methyl mercury and organic sulphur species in soil, soil solution and stream of a boreal forest catchment. Biogeochemistry 64, 53–76. https://doi.org/10.1023/A:1024904502633.

Smith-Downey, N.V., Sunderland, E.M., Jacob, D.J., 2010. Anthropogenic impacts on global storage and emissions of mercury from terrestrial soils: insights from a new global model. J. Geophys. Res. Biogeo. 115 https://doi.org/10.1029/2009JG001124.

Tarantilis, P.A., Pappas, C.S., Alissandrakis, E., Harizanis, P.C., Polissiou, G.G., 2012. Monitoring of royal jelly protein degradation during storage using Fourier-transform infrared (FTIR) spectroscopy. J. Apic. Res. 51, 185–192.

Úbeda, X., Lorca, M., Outeiro, L.R., Bernia, S., Castellnou, M., 2005. Effects of prescribed fire on soil quality in Mediterranean grassland (Prades Mountains, north-east Spain). Int. J. Wildland Fire 14, 379–384. https://doi.org/10.1071/WF05040.

Vega, J.A., Fernández, C., Fonturbel, T., 2005. Throughfall, runoff and soil erosion after prescribed burning in gorse shrubland in Galicia (NW Spain). L. Degrad. Dev. 16, 37–51. https://doi.org/10.1002/ldr.643.

Vieira, A.M.D., Vaňková, M., Campos, I., Trubač, J., Baieta, R., Mihaljevič, M., 2022. Estimation of mercury emissions from the forest floor of a pine plantation during a wildfire in Central Portugal. Environ. Monit. Assess. 194 https://doi.org/10.1007/s10661-022-10436-7.

Viscarra Rossel, R.A., 2008. ParLeS: software for chemometric analysis of spectroscopic data. Chemom. Intell. Lab. Syst. 90, 72–83. https://doi.org/10.1016/j.chemolab.2007.06.006.

Wang, X., Yuan, W., Lin, C.-J., Zhang, L., Zhang, H., Feng, X., 2019a. Climate and vegetation as primary drivers for global mercury storage in surface soil. Environ. Sci. Technol. 53, 10665–10675.

Wang, X., Yuan, W., Lu, Z., Lin, C.-J., Yin, R., Li, F., Feng, X., 2019b. Effects of precipitation on mercury accumulation on subtropical montane forest floor: implications on climate forcing. J. Geophys. Res. Biogeosci. https://doi.org/10.1029/2018JG004809.

Witt, E.L., Kolka, R.K., Nater, E.A., Wickman, T.R., 2009. Forest fire effects on mercury deposition in the boreal forest. Environ. Sci. Technol. 43, 1776–1782. https://doi.org/10.1021/es802634y.

Woodruff, L.G., Cannon, W.F., 2010. Immediate and long-term fire effects on total mercury in forests soils of northeastern Minnesota. Environ. Sci. Technol. 44, 5371–5376. https://doi.org/10.1021/es100544d.

Xu, J., Kleja, D.B., Biester, H., Lagerkvist, A., Kumpiene, J., 2014. Influence of particle size distribution, organic carbon, pH and chlorides on washing of mercury contaminated soil. Chemosphere 109, 99–105. https://doi.org/10.1016/j.chemosphere.2014.02.058.

Zheng, Y., Luo, X., Zhang, W., Wu, X., Zhang, J., Han, F., 2016. Transport mechanisms of soil-bound mercury in the erosion process during rainfall-runoff events. Environ. Pollut. 215, 10–17. https://doi.org/10.1016/j.envpol.2016.04.101.

Zhou, J., Obrist, D., Dastoor, A., Jiskra, M., Ryjkov, A., 2021. Vegetation uptake of mercury and impacts on global cycling. Nat. Rev. Earth Environ. 2, 269–284. https://doi.org/10.1038/s43017-021-00146-y.

Zhou, Z., Cao, X., Schmidt-Rohr, K., Olk, D.C., Zhuang, S., Zhou, J., Cao, Z., Mao, J., 2014. Similarities in chemical composition of soil organic matter across a millennia-old paddy soil chronosequence as revealed by advanced solid-state NMR spectroscopy. Biol. Fertil. Soils 50, 571–581. https://doi.org/10.1007/s00374-013-0875-6.